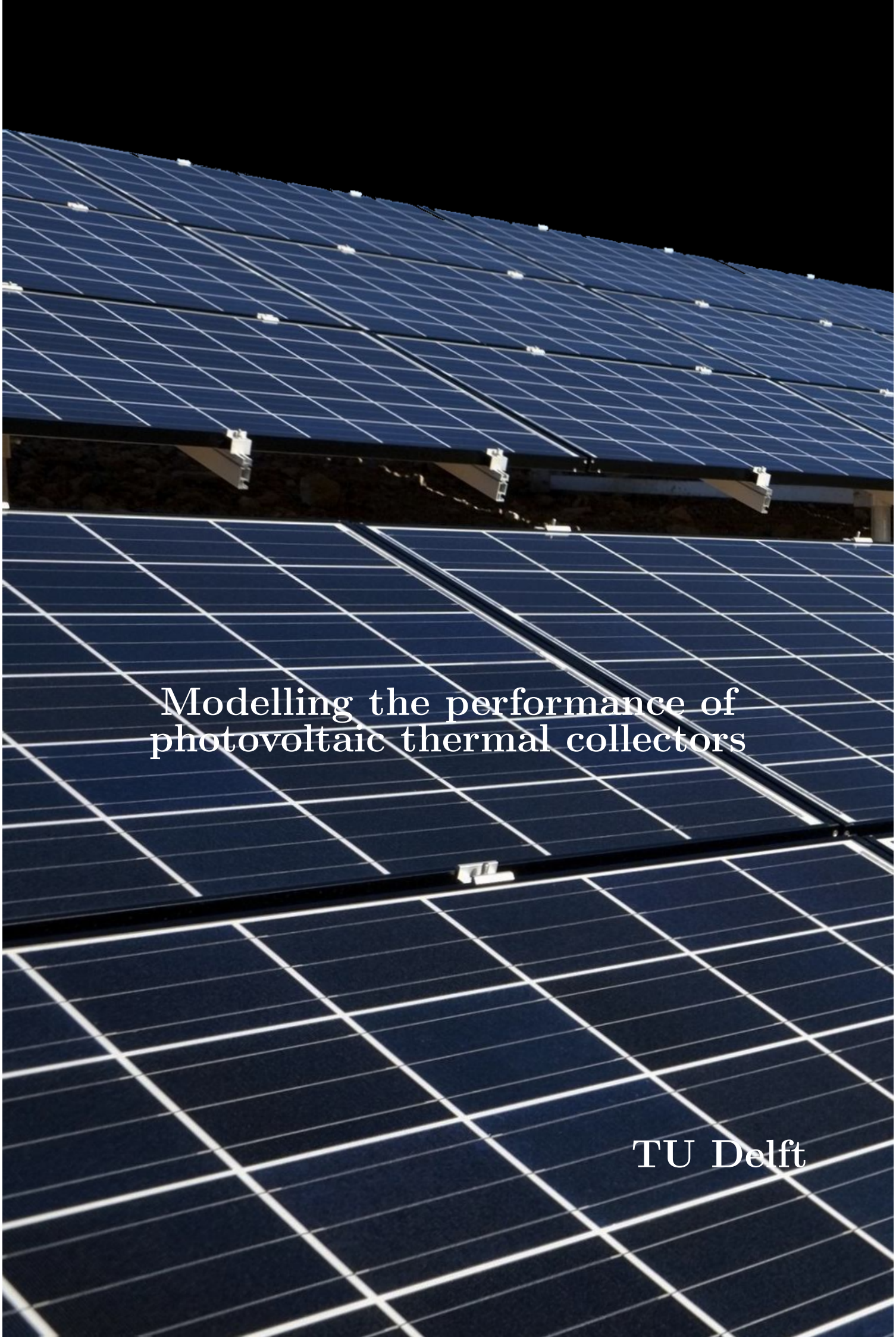

Modelling the performance of photovoltaic thermal collectors

TU Delft

Modelling the performance of photovoltaic thermal collectors

Thesis report

by

Jaap Dijkstra

To obtain the degree of Master of Science at the Delft University of Technology. To be defended publicly on

Thesis committee:

Daily Supervisor: Zain Ul Abdin

Project Duration: March 2023 - March 2024

Student number: 4600010

Sustainable Energy Technology (SET)
TU Delft
April 18, 2024

Preface

It is with pleasure that I present this thesis project, which marks the end of months of research, analysis, and writing. This work represents the last milestone in my academic journey, and I am grateful for the opportunity to undertake it.

The subject of this project, modelling the performance of photovoltaic thermal collectors, is one that has fascinated me throughout this period of time. Through my research, I have delved into the existing literature, consulted with experts in the field, and conducted my own calculations and analysis to arrive at the conclusions presented here. I hope that this project will contribute to ongoing discussions and debates in the field, and that it will inspire others to pursue their own research.

I would like to take this opportunity to express my gratitude to my thesis supervisors: Zain Ul Abdin and Rudi Santbergen for their guidance, feedback and support throughout this project.

Jaap Dijkstra

Student number : 4600010

Abstract

This thesis addresses a critical challenge in the field of renewable energy, focusing on the efficient utilization of Photovoltaic-thermal (PVT) systems. Much research has already been done on PVT and there exist many thermal simulation models. However, many of the researches done and existing thermal models are restricted to a specific collector archetype which gives less flexibility in experimentation between multiple archetypes. In addition, many experimental researches require a physical setup for measurements and thermal simulation models would need to be altered for different research approaches and collector archetypes. The primary objective of this thesis project is therefore to create a performance simulation framework model that is suitable for the calculation of the thermal and electrical performance for any PVT archetype. It aims to develop and implement a toolbox application encompassing heat transfer models that can establish a foundation for future research on PVT collector optimization, PVT system integration and PVT performance analysis. This toolbox application will be implemented into the PVMD Toolbox Vogt et al. (2022), housed within the Photovoltaic Materials and Devices research group at TU Delft.

Selected PVT collector: This research has visualized that there is a wide variety of PVT archetypes that can be used for current and future generations of PVT collectors. PVT collectors can be combined with heat pumps, refrigeration pumps, phase change materials and multiple forms of heat collection via fluids or air. These combinations can all contribute to high electrical and thermal efficiencies

Numerical heat transfer model and assumptions: It is possible to calculate heat transfer rates of complex designs when using a Finite Element Method (FEM) approach to calculate the heat transfer within the collector. With the proper convective and radiative equations to the environment, the heat transfer inside the collector and to the environment could be calculated without needing an experimental setup.

Performance calculations: The performance calculations gave insight into the simulated behavior of the PVT collector when operating in real-world conditions. Ranging the inclination angle from 0 to 60 degrees showed that the thermal efficiency became around 55% at an irradiance of 800 W/m^2 at 45 degrees. It also showed that differences in dimensions like pipe thicknesses and number of pipes did not affect the thermal performance that much. The daily performance calculations illustrated that the thermal energy lost to the environment can be three times as high as the incoming solar energy due to the low ambient temperatures compared to the inflow temperature. In the summer, PVT can achieve high total efficiencies of around 75% making PVT suitable during those times. The economic analysis showed that a PVT collector can have an LCOE of \$0.08/kWh which is lower than the \$0.13/kWh of conventional PV.

Contents

List of Figures

List of Symbols

α	Thermal expansion coefficient (Per Kelvin)
β	Thermal expansion coefficient (Per Kelvin)
Δ	Difference or change in a variable
$\dot{m}$	Mass per unit time (Kilogram per second)
$\dot{Q}$	Heat per unit time (Watts)
ϵ	Emissivity (-)
η	Efficiency (-)
η_{el}	Electrical efficiency (-)
η_{th}	Thermal efficiency (-)
η_{tot}	Overall efficiency (-)
μ	Dynamic viscosity (Pascal second or Kilogram per meter second)
ρ	Density (Kilogram per cubic meter)
σ	Stefan-Boltzmann constant (Watts per square meter per Kelvin to the fourth)
A	Area (Square meters)
Bi	Biot number (-)
c	Specific heat (Joules per kilogram per Kelvin)
D	Diameter (Meter)
E_b	Emissive power (Watts per square meter)
FF	Fill Factor (-)

Fo	Fourier number (-)
g	Acceleration due to gravity (Meter per second squared)
h	Heat transfer coefficient (Watts per square meter Kelvin)
I	Current (Ampere)
I_{sc}	Short circuit current (Ampere)
J	Radiosity (Watts per square meter)
k	Conductivity (Watts per meter Kelvin)
L	Length (Meter)
m	Mass (Kilogram)
Nu	Nusselt number (-)
P	Power (Watt)
Q	Heat (Joules)
Ra	Rayleigh number (-)
Re	Reynolds number (-)
T	Temperature (Kelvin)
V	Voltage (Volt)
v	Velocity (Meter per second)
V_{oc}	Open circuit voltage (Volt)

Chapter 1

Introduction and background information

After the agricultural and industrial revolution, the world is currently in the transition to the biggest revolution yet: The energy revolution. Our society is continually growing and thus its energy demand, rising it by an additional 30 percent relative to the consumption in 2016 by 2035 (Sathe and Dhoble (2017)). If the energy demand would still be covered by fossil-based energy sources, the resulting rise in Carbon Dioxide (CO_2) would lead to an unsustainable future. Research is therefore currently done on several alternative forms of sustainable energy generation. One of the currently popular forms of generation is Photovoltaic (PV) energy generation. Based on its modular design, PV energy generation can be performed on small or large scale for a range of applications. Over the years it has proven its capability of generating large amounts of electricity. However, it also has fundamental drawbacks.

Conventional PV systems operate on efficiencies of around 20 percent. The remaining energy will be produced as excess heat that will negatively impact the performance and lifetime of the PV modules if not conducted properly. Aside from PV, solar thermal systems transfer solar energy into heat that can be used for domestic space heating or other applications that require thermal energy. Both systems are essential for independent energy utilisation yet due to limited area on, for instance, rooftops of buildings, a combined installation of both systems would be impossible (Huide and et al (2017)).

Photovoltaic Thermal (PVT) collectors are a hybrid of both PV and solar thermal. PVT collectors are able to collect the generated excess heat of their PV solar cells in order to minimize the reduction of the electrical efficiency and gain additional thermal energy. The overall efficiency of the entire system can therefore be vastly increased. There is already a growing global market for PVT collectors though not as large compared to regular PV, as can be seen in Figure 1.1. Development and optimization on PVT modules is therefore crucial for future generations of solar energy generation technology and the energy transition.

PVT technology is available since 1975 but the global installed power began significantly rising around 2008, of which most common were flat-plate glazed PVT modules with water as heat extraction medium (AEE_INTEC (2021)). In the years after that, many alternatives of PVT configurations and thermal collector media were researched upon.

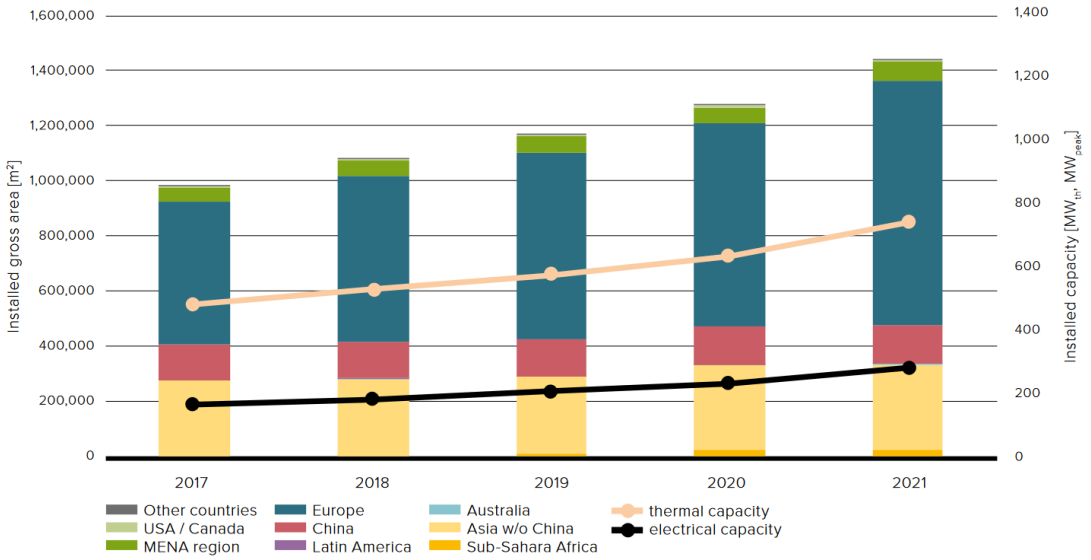

Figure 1.1: Global market development of PVT collectors from 2017 to 2021 (AEE_INTEC (2021))

1.1 PV and solar thermal modules

As previously mentioned, one of the currently popular forms of sustainable energy generation is using PV modules. The most commonly used semiconductor material for this is silicon. Silicon can only use light with wavelengths between 300 nm and 1200 nm for the photovoltaic effect. Typically, a single junction solar cell can only utilize a maximum of 33% of the incident light to produce electricity due to the Shockley-Queisser limit (SQL) (Smets and et al (2016)),(Shockley and Queisser (2004)). The band gap of silicon and the SQL can be seen in Figure 1.2 and Figure 1.3 respectively.

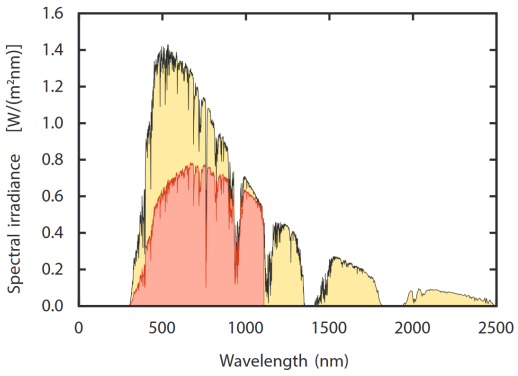

Figure 1.2: Band gap of silicon (red) versus AM1.5 solar spectrum (Smets and et al (2016))

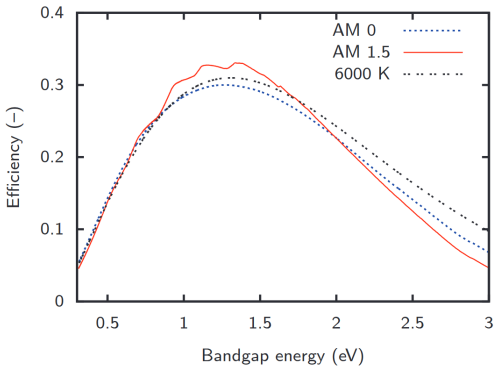

Figure 1.3: SQL for different irradiance spectra (Smets and et al (2016))

In general, more than 80% of solar radiation will be converted to heat. Research shows that a PV cell's electrical efficiency decreases by 0.09% for every degree rise in cell temperature for single junction c-Si solar cells (Singh (2012)), 0.05% for hetero-junction silicon solar cells (Bätzner (2011)) and 0.05% for multi-junction InGaP/GaAs/G solar cells (Or (2014)). This loss in efficiency would be impactful in hot climates or during summer. To counter this, PVT collectors are able to collect the generated heat to keep the PV cells at low operation temperatures when supplied by a heat extraction medium with a lower temperature than that of the PV cells and utilises the otherwise excess heat for thermal storage or other applications. An overview with general information about PVT collectors and useful applications for this type of collectors will be explained in the next section.

1.2 General information about PVT collectors

Working principle of PVT collectors: A PVT collector typically consists of photovoltaic cells of semiconductor material, a thermal collector with a heat extraction medium and a heat exchanger between the collector and the used application or thermal storage container. The semiconductor material converts sunlight into electricity while the thermal collector absorbs the generated heat resulting from this conversion. The heat absorbed by the thermal collector will then be transferred to the extraction medium, which can then be transferred via the heat exchanger to a suitable low grade heat storage tank or for direct use. A simplified schematic of a PVT system combined with a heat pump can be seen in Figure 1.4 for better visualization.

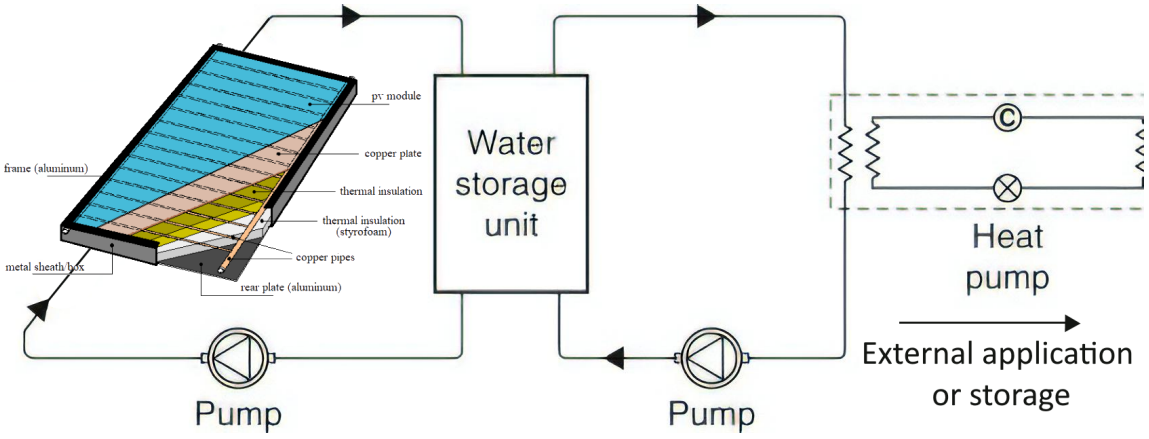

Figure 1.4: Example of PVT system (Kalogirou (2014))

The schematic above would be used for a flat-plate glazed liquid based collector. While this is the most apparent archetype of PVT collector installed today, many more archetypes and heat extraction media are possible for PVT technology which increases the number of options and applications to which PVT can be used for. These different archtypes will be presented and discussed upon explaining their respective advantages and disadvantages in section 1.3.

Applications for PVT: The thermal output of PVT systems can be used for a range of applications. These differ from small to large scale, low temperature to high temperature and in addition from short term to long term storage options. Some examples would be the following:

- Air based, water based and bifluid PVT systems can be used for domestic or commercial space heating at low temperatures (Sathe and Dhoble (2017)).

- Domestic houses represent a high potential to produce energy for self-consumption or share it in an energy community at medium temperatures. The extra heat produced ban be stored in a tank and used for sanitary and heating (Abdin and Rachid (2021)).

- Public buildings and commercial sites can use PVT collectors for self consumption and sharing within the energy community for both heat and electricity at a large scale (Abdin and Rachid (2021)). Example sites may be public swimming pools or greenhouses.

- District heating and PVT can be combined at an entry point of district heating to inject the heat collected by PVT installations locally for the plant or be used as a complementary source generally through a heat pump to maximize efficiency (Abdin and Rachid (2021)).

- Industrial applications like drying and desalination have very intensive energy consumption. Solar plants with PV/Ts have been proven to be useful and efficient for such processes with high temperatures (Abdin and Rachid (2021)).

- PVT collectors in combination with heat pump storage can be used for cooling purposes in hot climates or during summers (Sathe and Dhoble (2017)). The heat from solar irradiation that would normally heat up rooftops and walls would now be collected and transferred to storage vats or underground storage, this heat can be used again during winter for space heating as previously mentioned.

- PVT can be used when heating or cooling is needed in solar farms to maximize the efficiency of land use. This may be the case for agroindustrial factories (Abdin and Rachid (2021)).

1.3 Different archetypes of PVT collectors

PVT collectors can be classified firstly in terms of module archetype, then into type of heat extraction medium and subsequently into their respective type of design. Figure 1.5 gives an overview chart of currently common types of PVT collectors.

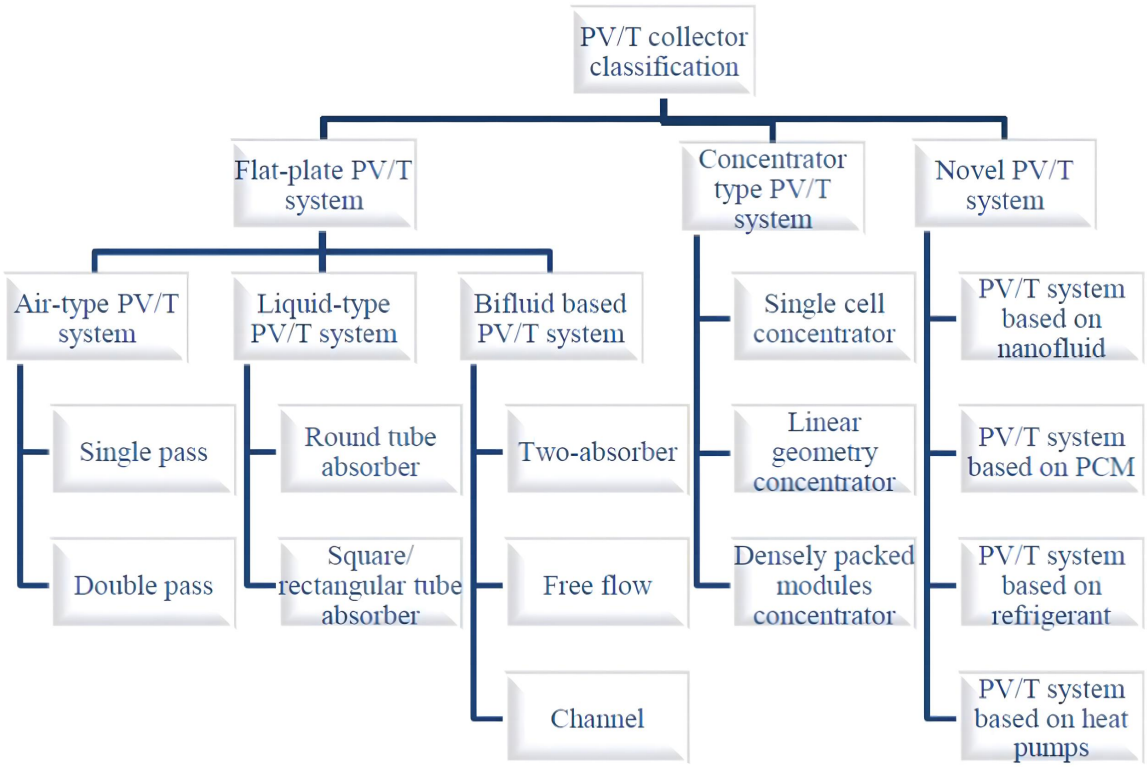

Figure 1.5: Classification of PVT collectors (Jia and et al (2019))

Each different collector archetype is more suitable for different applications and system sizes than others. The archetypes mentioned in the chart will therefore be briefly explained and the differences between them. An overview of the efficiencies of these archetypes will be visualized in section 1.5 according to research done upon them.

1.3.1 Flat-plate collectors

Flat-plate collectors are the most conventional archetype of PVT collectors. Most systems utilising this archetype are used for energy delivery at moderate temperatures. Flat-plate collectors utilize solar energy by direct and diffuse solar radiation without tracking the sun (Duffie and Beckman (2013)). The topology is quite similar to conventional PV modules. Flat-plate PVT is used widely in solar water heating, building and domestic space heating, air conditioning and industrial processes like drying. The construction of Flat plate PVT is simple and requires little maintenance. It is commonly integrated as part of a wall body or on rooftops, making the orientation fixed (Duffie and Beckman (2013)). The collector consist the PV cells that can either be glazed or unglazed and can be encapsulated by an insulation layer on the back and sides. The heat extraction medium can flow above or under the PV cells in either ducts, pipes, channels or gaps. The most common types of heat extraction fluids used are water and air either combined or by themselves.

- **Air based:** One of the current heat extraction mediums used for building heating is air based PVT. For this, regular PV modules could be used and air gaps could be made above or under the module. There are systems that use single pass or double pass ducts for optimised heat transfer. In Figure 1.6, some general configurations can be seen.

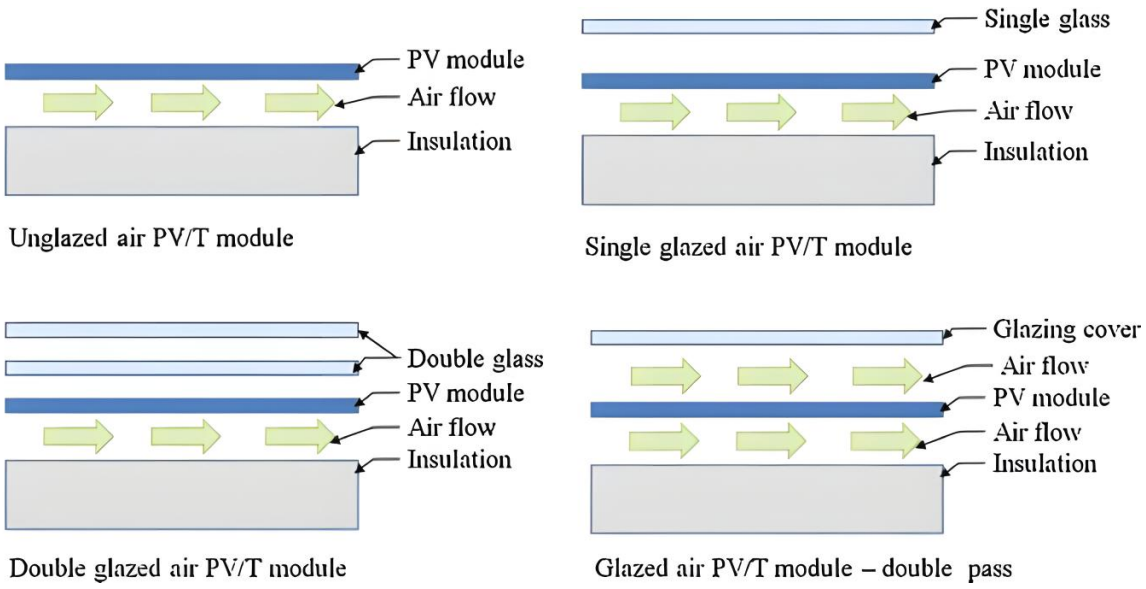

Figure 1.6: Cross section of air based PVT configurations (Zhang and et al (2012))

As seen in the figure, The PV cells can be cooled from both sides. This can be done through forced or natural convection if the module is mounted vertically on a wall. Air as a heat extraction medium is a rising trend with tall buildings since it can also serve for air circulation through the building due to natural convection.

Advantages of using air for PVT is that the design of such a system is simple and has low maintenance costs (Jia and et al (2019)). Disadvantages of using air as a medium is that it has a low thermal performance, that there are almost no industrial applications for hot air except for agricultural industry and that a large volume of air is needed for a successful heat transfer process (Jia and et al (2019)) and (Zhang and et al (2012)).

- **Liquid based:** Liquid based flat-plate PVT uses the same principle as air based PVT. Water is mostly used since it is cheap to use and it has a high heat capacity. In general, the extraction fluid is pumped through tubes or ducts. Different tube layouts can be designed with optimized surface area to maximize heat transfer from the collector to the extraction medium. A few tube design layouts for liquid based PVT can be seen in Figure 1.7, Figure 1.8 and Figure 1.9.
  If the temperature of the liquid remains lower than the cell temperature, the PV cells will be cooled. This will lead to a higher electrical efficiency. In the meantime, the passing fluid will be heated by absorbing the excess heat and can be stored or directly used. Compared to the air-based system, the water-based PV/T systems could achieve the enhanced cooling effectiveness due to higher heat capacities like that of water and therefore both the thermal and electrical efficiencies of the systems would be higher than air based systems (Zhang and et al (2012)).

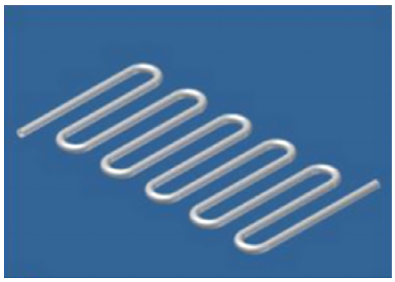

Figure 1.7: serpentine absorber (Fudholi and et al (2014))

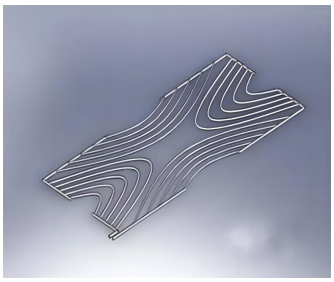

Figure 1.8: web flow absorber (Fudholi and et al (2014))

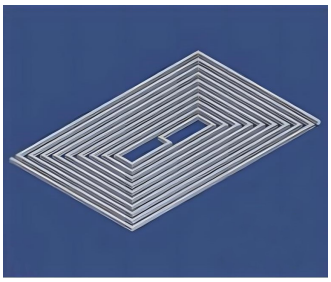

Figure 1.9: spiral flow absorber (Fudholi and et al (2014))

Advantages of using a liquid as a heat extraction medium is that it can use fluids with a high heat capacity, designing liquid based systems have low costs and a heated extraction fluid like water can have a direct contribution.
Disadvantages of liquid based systems is that it is a more complex system to install in contrast to air based systems. During winters it is possible that the pipes can freeze so antifreeze would be required in cold climates (Zhang and et al (2012)). Another disadvantage is that hot water used for high heat technical applications should be necessary to operate at least around 40–50 °C. However, such a temperature might penalize the electric performance of the PV cells. On the other hand, lower temperatures would allow better electrical efficiency, but they would also affect the usefulness of the recovered heat (Tiwari (2002)). A compromise must therefore be made in certain applications.

- **Bifluid based:** Bifluid collectors enable to simultaneously produce hot air, hot water and electricity altogether to overcome limitations of individual air based PVT and water based PVT systems. The PV cells could be for instance cooled on the front by air ducts and cooling fins and cooled at the back by water tubes. This makes it possible for the PVT collector to simultaneously collect water for central heating and use the hot air for air circulation in the building. An example design of a bifluid collector can be seen in Figure 1.10.

  Advantages of bifluid PVT would be higher heat gains and efficiencies due to better cooling than having separate PVT systems (Awad (2022)). A disadvantage would be the interdependence between the water and air circulation. (Jarimi and et al (2016)) observed that in bifluid mode, as the mass flow of one medium increased, the thermal efficiency of other medium tends to decrease.

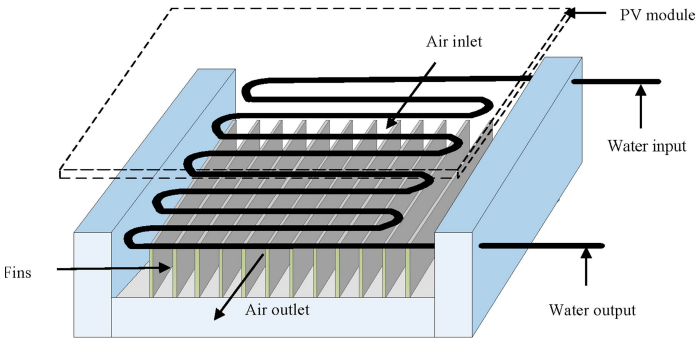

Figure 1.10: An example of a bifluid PVT collector (Jarimi and et al (2016))

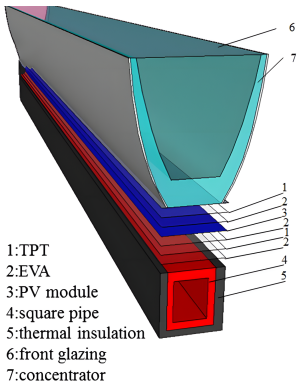

Figure 1.11: Schematic of a typical concentrated PVT module (et al (2015))

1.3.2 Concentrated PVT collectors

In contrast to regular Flat-plate collectors, Concentrated PVT collectors redirect solar radiation to the PV cells by the use of mirrors. With this concept, less cell area is needed which reduces manufacturing costs (Fikri and et al. (2022)). Types of concentrators would be a parabolic reciever, a Fresnel-lens or linear Fresnel reflectors. in Figure 1.11, a parabolic topology can be seen. Concentrated PVT can use the same heat extraction media that are used for flat-plate PVT collectors.

Advantages to Concentrated PVT are: The thermal efficiency is high because of the small heat loss area relative to the receiver area. Reflecting surfaces require less material and are structurally simpler than Flat-plate collectors. For a concentrating collector the cost per unit area of the solar collecting surface is therefore less than that of a Flat-plate collector. Owing to the relatively small area of the receiver per unit of collected solar energy, selective surface treatment and vacuum insulation to reduce heat losses and improve the collector efficiency are economically viable (Tyagi and et al (2012)).

Disadvantages to Concentrated PVT are: Concentrator systems collect little diffuse radiation depending on the concentration ratio. Some form of tracking system is required so as to enable the collector to follow the sun's trajectory. Solar reflecting surfaces may loose their reflectance with time and may require periodic cleaning and refurbishing (Tyagi and et al (2012)).

1.3.3 Novel PVT collectors

- **Nanofluid based collectors** Nanofluid based collectors generally contain nano-particles of sizes less than 100 nm in heat extraction fluids like water, glycol and oil. Nanofluids are basically improved heat extraction fluids and thus can be used efficiently in various solar energy conversion systems (Sathe and Dhoble (2017)). In contrast to regular liquid based PVT collectors, properties of nanofluids can be enhanced for particular applications depending on the nanoparticle type, volume fraction of nanoparticles and base fluid. Nanofluid can be made to have, for instance, anti-freeze properties, making a PVT collector applicable in cold climates. The heat absorption coefficient can be increased as well for better thermal capacity.

  Advantages of nanofluid PVT is that it enables high electrical and thermal performance and that it makes it able to research different nanofluids that are tailored for certain applications. There are two major disadvantages about nanofluid technology. Firstly, despite huge investments in nanofluid technology for photovoltaic thermal systems, researchers still find it hard to achieve stable nanofluids during preparation (Sathe and Dhoble (2017)). Secondly, nanofluid technology is currently only experimental and highly expensive, making it yet unsuitable for the market.

- **Phase Change Material based collectors** Phase Change Materials (PCM) absorb thermal energy as latent heat at a constant temperature. PCM, with a suitable phase transition temperature, can be used to regulate the temperature of PV cells thus maintaining high efficiencies for an extended period of time. Compared to other methods of temperature regulation, the use of PCM has the added advantage of locally storing thermal energy that can be used asynchronously (Browne and et al (2015)). PCM can consist of low temperature PCM or high temperature PCM dependent on the application. A PCM collector configuration can be seen in Figure 1.12. The materials used for PCM can be devided between organic an inorganic materials, each with their respective advantages and disadvantages.

  Advantages of using organic PCM is that no corrosive material has to be used, there is no or low undercooling and it is chemically and thermally stable during operation. The major advantage of inorganic PCM to organic is that it can have a far greater phase change

enthalpy, making it capable of storing more heat than organic material. Disadvantages of organic PCM are a low thermal conductivity and inflammability. A disadvantage of inorganic PCM is that they are often corrosive materials (Browne and et al (2015)). An overall disadvantage of using PCM is that if the PCM is saturated, it decreases the thermal performance of the collector (Awad (2022)).

- **Heat pump and refrigerant based collectors** Plain water or air based PVT collectors have the disadvantage that they are restricted to a certain operation temperature either set by their application or storage container. Heat pump and refrigeration cycles are often used to manipulate the temperature of the heat extraction medium to maximize the thermal output. A heat pump based PVT system can be seen in the previously mentioned Figure 1.4.
  The heat extraction medium can exchange its heat with the heat pump working medium via a heat exchanger. This medium can be compressed via a compressor for high temperatures to exchange heat with a thermal storage container and then expanded via an expansion valve to reach low temperatures for the heat collection of the PVT collector. Heat pump cycles also have a high potential for underground water storage as can be seen in Figure 1.4. The excess heat can then be stored during summer and extracted during winter.

  Advantages of heat pump and refrigerant systems are that the operating temperature of the heat extraction medium can be manipulated so that the output temperature can be changed for its respective application and the PV cells can be cooled to low operation temperatures for higher electrical efficiencies. Disadvantages of these systems are that the overall system would be quite expensive compared to other PVT collector types and refrigerant fluids can be toxic to the environment if there would be a leakage in the system.

- **Heat pipe based collectors** Heat pipe based collectors are considered efficient heat transfer collectors that combine the principles of both thermal conductivity and phase transition. A typical heat pipe consists of three sections namely, evaporated section (evaporator), adiabatic section and condensed section (condenser), and provides an ideal solution for heat removal and transmission (Zhang and et al (2012)). In contrast to normal liquid based systems, heat pipes can be used in colder climates since it is not necessarily dependent on the outside air temperature. A sketch of a heat pipe module can be seen in Figure 1.13.

  Advantages to heat pipe based collectors are that they are operational during all seasons, heat pipe solar thermal collectors are already developed and globally used and a heat pipe system is relatively affordable in contrast to other PVT collector technologies (Sathe and Dhoble (2017)). A disadvantage could be that a heat pipe based system is dependent on the capacity of the thermal energy storage container required for the system.

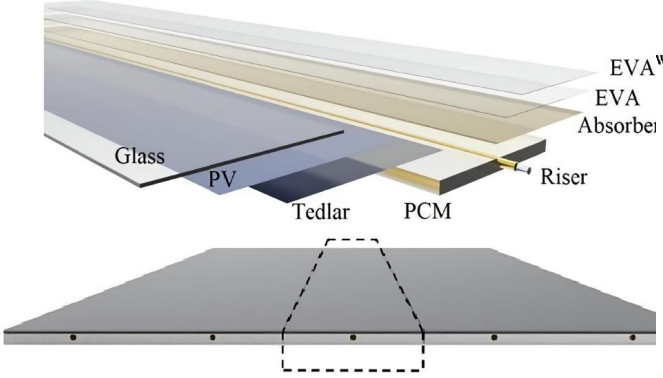

Figure 1.12: An example of a PCM PVT collector (Kazemian and et al (2020))

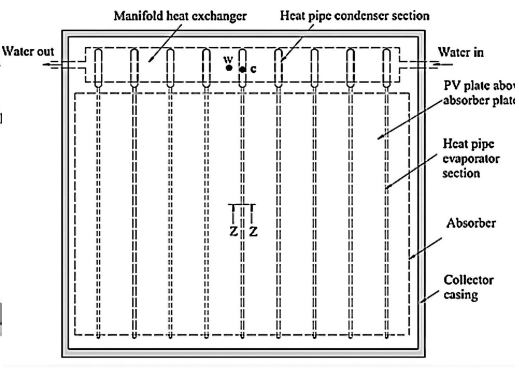

Figure 1.13: Schematic of a heat pipe based PVT collector (Wu and et al (2011))

1.4 Challenges and disadvantages of PVT

Even though PVT technology has potential of becoming a future way of photovoltaic energy generation, it still needs substantial improvements to become competitive in contrast to the already proven PV and solar thermal technologies (Sathe and Dhoble (2017)). Firstly, there is a lack of public awareness on PVT technology. PV and solar thermal are already well accepted and promoted by the public and governments but PVT is still in its primary stage (Sathe and Dhoble (2017)). Since PVT collectors are not as integrated in the public market as regular PV, many issues concerning their design, the market potential and possible barriers for their practical application are still being investigated (Evola and Marletta (2014)). Secondly, under highly concentrated operating conditions or without a uniform illumination, operation of PVT systems can become unstable (Jia and et al (2019)). Thirdly, the application of a PVT system highly depends on its climatic situation. PVT can be useful during summers but additional energy input is needed during winter to satisfy the energy demand of applications like central heating (Jia and et al (2019)). Long term seasonal thermal storage has been mentioned as a solution to this problem but an effective storage solution has yet to be made.

1.5 Research gap

Much experimental research is done on PVT and there exist several thermal simulation models that are able to calculate the performances of different PVT collector archetypes and heat extraction media which can be found in Table 1.1. However, many of those are either restricted to a specific collector archetype, heat extraction medium or design, giving less flexibility in the experimentation and optimization between different archetypes and design parameters. While experimental research can be helpful for measuring realistic PVT collector performances and existing thermal simulation models for complex designs, it is unfeasible to research in optimization with differences in, for instance, collector archetypes, collector dimensions and conduction materials, since the whole system has to be rebuild for the experimental setup or the thermal simulation model has to be altered. (Zondag (2003)) started with combining theoretical 1D, 2D and 3D models with experimental setups where the models would be used for collector optimization and the experimental setup would validate if the simulation models are realistic. The research concluded that while the 1D model works several times faster than the 2D and 3D model, each model required long calculation times so simplifications had to be made for its reduction. In addition, a physical test setup of the module was still necessary to measure and determine the heat transfer going to the collector side of the module. A universal flexible simulation framework for PVT performance calculation is therefore needed to enable further research on PVT optimization and performance comparison between collector archetypes.

Table 1.1: Table with research output values

Archetype	medium	area m^2	η_{th}%	η_{el}%	η_{tot}%	research	location
Flat-plate	water	0.944	64.00	12.00	76.00	Dupeyrat (2011)	Switzerland
Concentrated	nanofluid	1.200	-	-	21.20	An (2016)	China
Flat-plate	air	1.620	42.00	8.40	50.00	Solanki (2009)	Netherlands
Flat-plate	air	0.640	54.70	10.00	64.70	Jin (2010)	Malaysia
Flat-plate	heat pipe	-	63.35	8.45	71.00	Wu (2011)	model
Concentrated	nanofluid	0.146	48.10	12.51	60.61	Ju (2020)	model
Concentrated	nanofluid	0.010	79.40	5.48	84.88	Han (2020)	China
Flat-plate	water	0.985	29.35	9.99	39.19	Awad (2022)	Iraq
Flat-plate	bifluid	0.985	49.05	9.96	59.01	Awad (2022)	Iraq
Flat-plate	bifluid+PCM	0.985	69.23	11.06	80.29	Awad (2022)	Iraq
Cov. Flat-pl.	water	0.940	54.00	6.70	60.70	Zondag (2002)	Netherlands
Uncov. Flat-pl.	water	-	52.00	9.70	61.70	Zondag (2003)	model
Cov. Flat-pl.	bifluid	-	65.00	8.40	73.40	Zondag (2003)	model

At the Technical University of Delft a digital toolbox is currently in development by the Photovoltaic Materials and Devices (PVMD) research group. This toolbox accurately simulates the electrical performance of a PV module for a vast amount of input design values using mathematical models based on current research on PV. In order to get a complete picture of the overall performance including thermal performance however, a toolbox application that calculates the thermal performance is needed as well. Because the toolbox is required to perform all simulations in MATLAB (MathWorks (2021)), a toolbox application specialized for PVT collectors has to created in that environment.

1.6 Research objective

The primary objective of this thesis project is to create a performance simulation framework model that is suitable for the calculation of the thermal and electrical performance for any PVT archetype. To achieve this overarching goal, this research will focus on the following sub-objectives:

- **Sub-objective 1: Choosing a reference collector**
  Here, out of the presented PVT collectors one will be chosen as a reference collector for the validation of the simulation results.

- **Sub-objective 2: Formulating the PVT heat transfer calculations**
  This entails the development of Finite Element Method (FEM) mathematical models to simulate the thermal behavior of the collector, providing a theoretical framework for PVT performance analysis.

- **Sub-objective 3: Validating simulation output**
  To validate the simulation output of the model, the results must be verified with the results of a measurement experiment with a similar PVT collector.

- **Sub-objective 4: Simulating PVT collector performances**
  The final steps involve daily performance simulations and cost-effectiveness assessment to provide insights on the results the model provides on the operational dynamics of a PVT collector within real-world conditions.

These sub-objectives lay the groundwork for a comprehensive analysis, from initial assessment to practical evaluation, ensuring a thorough exploration of the potential benefits of integrating PVT technology.

After reaching its objectives, this project will integrate these models into the PVMD Toolbox. This framework establishes the foundation which can expanded upon for PVT collector optimization research, archetype experimentation, PVT system integration, environmental PVT performance analysis and for economic sustainability analysis, facilitating the development of more efficient and sustainable energy solutions.

1.7 Structure

The structure of this thesis report is as follows: firstly, in chapter 2 the selection of the collector used as a reference for validation of the model will be presented. Secondly, in chapter 3 the mathematical heat transfer equations for this chosen collector will be explained. Thirdly,chapter 4 will validate the model with measured reference values accompanied by a sensitivity analysis. After that, chapter 5 will show a daily performance simulation and a yearly performance simulation with a Levelized Cost of Electricity (LCOE) analysis to give insight in the yield and costs of a PVT collector. Chapter 6 discusses the results obtained. Lastly, chapter 7 and chapter 8 respectively covers the conclusion and recommendations about the research.

Chapter 2

Reference collector selection

Out of the different PVT collectors that are presented, one will be chosen as a reference collector for the FEM heat transfer calculations. While the main goal of this research is to make the model suitable for any archetype a single collector archetype will be sufficient for the model validation. It is not within the scope of this research to implement every previously presented archetype into it. The aim of this chapter will be to select an archetype that includes a simple design that is easy to implement in the FEM models, utilises commonly used heat extraction fluids and collector materials, has available empirical performance data and has flexibility in modification with the collector dimensions and design topology. All previously stated PVT collectors will be discussed regarding these requirements going down from collector archetype to heat extraction fluid to design topology and one will be selected as the reference collector.

2.1 Archetype

- **Flat-plate:** Flat-plate PVT collectors are the most commonly used archetype out of the the three archetypes that are mentioned in this research. Commercial collectors already exist with a wide variety in collector design and heat extraction media. Much empirical research has already been done on these types of collectors and it is a suitable candidate for performance optimization research. Because of the possibility to use simple designs and commonly used materials and media like copper, aluminium, water and air it is a suitable candidate as a reference collector archetype. In addition, the flat-plate archetype is highly modifiable with its conduction materials and heat extraction fluids.

- **Concentrated:** Concentrated PVT collectors are structurally simpler than flat-plate collectors so a simple design could be used as a reference collector in the model. However, because the principle of the concentrator archetype lies in the reflection of incoming sunlight, ray-tracing calculations for the irradiance and light absorption would be required in addition to the heat transfer equations that have to be formulated for the performance simulation. This would unnecessarily further the scope of this research because for flat-plate archetypes irradiances and absorption values are already available from previous empirical research on PVT and PV and do not vary when the dimensions and design changes in the model. A Concentrated PVT collector would therefore be less suitable as a reference archetype for the framework model but the model can be expanded upon to include ray-tracing formulas.

- **Novel:** While the novel archetypes can lead to high total efficiencies and can improve the performance of already existing PVT archetypes by combining technologies or enhancing heat extraction media, the technologies are still mostly in an experimental stadium. Most existing researches on these archetypes are lab experiments and not measurements of conventionally used PVT collectors. high performance PVT collectors are either still

too expensive too be implemented in the market or use unstable or hazardous fluids and materials. Experimentation and optimization with these archetypes would require thorough additional research on these topics and the including dangers for some archetypes in addition to the heat transfer equations so they would not be a suitable candidate for a reference collector in this research.

2.2 Heat extraction medium

- **Air based:** Air based collectors are easy to implement and would require only the heat transfer calculations in the model to calculate the performance of the collector. since regular air can be used as heat extraction medium and for the losses to the environment an air based collector would be a sufficient candidate as a reference collector. However, air based PVT collectors are mostly limited to low temperature applications with overall low thermal efficiencies and are mostly used for space heating and air circulation. Because the aim of this research is to make a model that would be a framework for performance optimization research, having a collector capable of reaching high thermal efficiencies would be a requirement.

- **Liquid based:** Liquid based PVT collectors using water are well presented in the field of PVT as can be seen in Table 1.1. It has a high potential for combination possibilities with other collector archetypes and modification in design plus being capable of reaching overall high efficiencies. In addition, a lot of research has been done on liquid based collectors including the already existing numerical simulation model from (Zondag (2002)) which has both a simulation model and empirical measurements that can be used for the validation of the model. The required materials for a liquid based collector can be conventionally used materials like copper and aluminium. A liquid based collector would be a suitable reference collector.

- **Bifluid based:** Bifluid based collectors share the same attributes with air based and liquid based collectors. The high potential of bifluid for combinations with other collector types and heat transfer makes it a good candidate. The combination of water pipes under the PV cells and free flowing air over the cells while the module is covered can give roughly an additional 20% as seen from the experiment from (Awad (2022)) in Table 1.1. While Bifluid based collectors would be capable of reaching high thermal efficiencies in combination with better cooling for the PV cells the interdependence between water and air would require additional sensitivity research on the their influence on their respective thermal efficiency before validation. Having therefore only one of the two as a heat extraction medium for the reference collector would be more suitable.

2.3 Thermal collector design

- **Serpentine absorber:** The most used tube design is the serpentine absorber layout. It is relatively easy to produce and it is accessible for modification in pipe diameter and spacing. In this layout, water is gradually heated up and there is no mixing with water with lower temperatures. This would be the simplest design to implement in the model.

- **Web flow absorber:** Web flow absorbers split up the main water tube into various smaller tubes for a higher heat transfer surface area. This could prove useful in optimizing the heat transfer and in addition the overall efficiency of the system. The design is more complex to implement in the model.

- **Cooling fins:** When bifluid or air is used, cooling fins are needed to optimize the heat transfer from the PV cells to the air. The fins could be used as ducts under the water tube

collector to prevent heat losses from the back of the system or between the PV cells in a covered system to help cool the PV cell from the top. Cooling fins would be required in the design if the reference collector would be air based or bifluid based.

- **Ducts:** Instead of using tubes, water can also flow trough multiple ducts under the PV cells. Wide flat ducts have a higher surface area for heat transfer in contrast to tubes and could have a compact design. It is therefore worth investigating the performance of designs using this layout. This design is roughly similar to the serpentine absorber except that the serpentine absorber would consist out of a single tube.

- **Covered or uncovered:** As mentioned previously, a PVT collector can be covered or uncovered on the top. An uncovered collector could be cooled by natural or forced convection from the outside wind or rain, but that heat cannot be recovered and is therefore lost. A covered system would have a higher resistance to losses from the top or can be cooled from the top by for instance air that can be recovered when a bifluid collector would be chosen.

2.4 Selected reference collector

The reference archetype is chosen to be a glazed-covered flat-plate PVT collector that is water cooled at the back of the module with a serpentine absorber design. Flat-plate archetypes are already commercially used which makes these archetypes interesting for optimization research and PVT system integration research. The collector design is simple to implement in the heat transfer model. The collector requires commonly used conduction materials and heat extraction fluids like copper, aluminium and water and is modifiable with other materials and dimensions. In addition, this reference design is used for the theoretical and experimental model in (Zondag (2002)) which provides empirical data that can be used for the validation of the model. An overview of the reference collector can be seen in Figure 2.1 and Zondag (2002) from the previous research. The dimensions of the collector that will be used in the model simulations are visualized in Table 2.1 and Table 2.2.

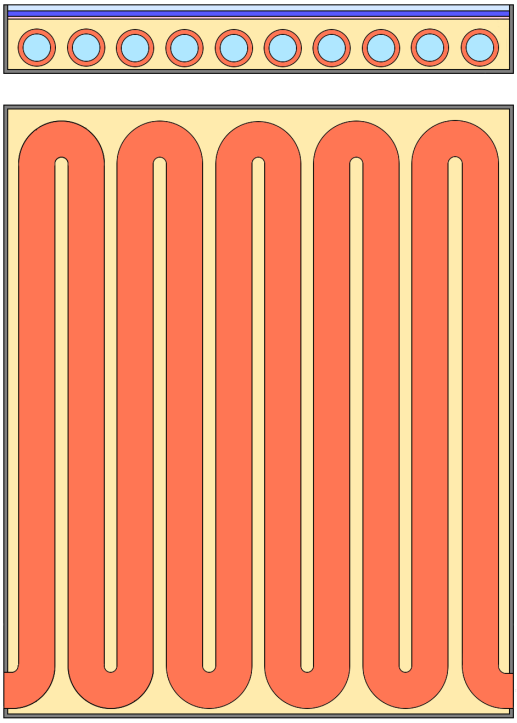

Figure 2.1: Top view and cross section selected PVT archetype

Table 2.1: Reference collector dimensions

Parameter	**Value**
Absorber area (A_{abs})	1.12 m^2
PV panel area (A_{pv})	0.94 m^2
Bond width (B)	0.01 m
Outer diameter tube (D)	0.01 m
Inner diameter tube (D_{inner})	0.008 m
Height insulating air layer (H)	0.02 m
Length tube segment (L)	0.724 m
Length of collector surface (L_c)	1.776 m
Tube spacing (W)	0.095 m

Table 2.2: Reference collector thicknesses

Parameter	**Value**
Thickness cover glass ($\delta_{topglass}$)	0.0032 m
Thickness air gap (δ_{air})	0.02 m
Thickness PV glass ($\delta_{pvglass}$)	0.0015 m
Thickness EVAt (δ_{pvEVA})	0.0015 m
Thickness PV (δ_{pv})	0.0035 m
Thickness EVAb (δ_{pvEVAb})	0.0015 m
Thickness TED ($\delta_{pvglass}$)	0.001 m
Thickness ad (δ_{pvad})	0.001 m
Thickness cu (δ_{pvcu})	0.002 m

2.5 Conclusion

The objective of this chapter was to select a simple reference PVT collector that is easy to implement in the FEM model. The selected reference collector will be used to validate the accuracy of the performance calculations done by the FEM heat transfer model. The selected collector is suitable because it is simple to implement into the model, requires commonly used materials, is modifiable and is commercially used which makes it interesting to expand upon for optimization research and PVT system integration research. The same collector is used in previous research with empirical data that can be used as well for the model validation.

Chapter 3

Numerical heat transfer model and assumptions

The goal of this chapter is to define the heat transfer equations necessary for the performance calculations of the previously selected PVT collector. Because three-dimensional analytical heat transfer calculations would quickly become complex and require much time for the calculation, the heat transfer within the collector will be calculated using a FEM approach for the models. The collector will be viewed as a matrix consisting out of interconnected material points that will represent a specific material with an area of influence shaped like a block. Between these points linear heat transfer calculation will be performed considering the energy conservation principle. The heat transfer through the collector and to the environment can then be numerically calculated. A 2D representation of the FEM approach can be seen in Figure 3.1

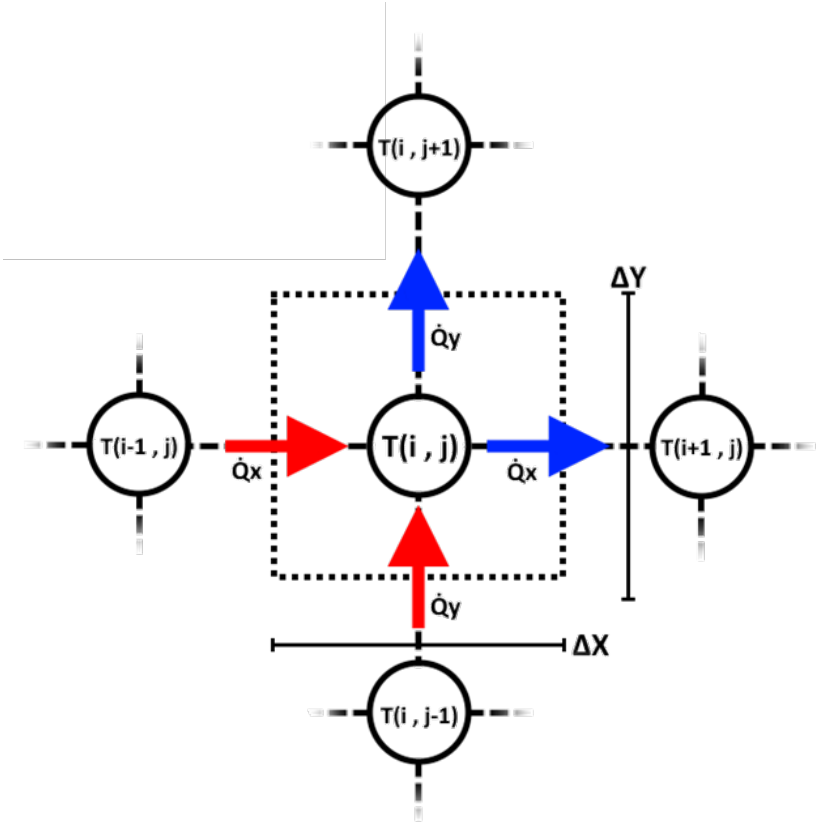

Figure 3.1: Unsteady state heat transfer

In the figure, it can be seen that the approach of simplifying an otherwise complex geometry into finite points that each represent a cubical volume will speed up calculation time and make the model flexible to use for any type of collector design as long as it can be represented in a matrix. On each side of the cube, linear heat transfer between the central point and its neighbouring point will be calculated. For this heat transfer, the following formula is used:

$$\rho \cdot Cp \cdot V \cdot \frac{dT(y,x,z)}{\Delta t} = \dot{Q}_{X\text{in}} + \dot{Q}_{Y\text{in}} + \dot{Q}_{Z\text{in}} + \dot{Q}_{X\text{out}} + \dot{Q}_{Y\text{out}} + \dot{Q}_{Z\text{out}} \tag{3.1}$$

This equation represents the energy balance within a control volume of the block of material for unsteady heat transfer. In the case steady heat transfer has to be calculated, the left term of the equality sign would be zero. The unsteady and steady cases will be explained in section 3.1 and section 3.2 respectively. The variables in the previous equation are defined as follows:

- ρ denotes the density of the material.
- Cp represents the specific heat capacity of the material.
- V stands for the volume of the block.
- $\frac{dT(y,x,z)}{\Delta t}$ is the rate of temperature change of the bulk temperature of the block, where x,y and z denote the spatial coordinates within the system.
- $\dot{Q}_{X\text{in}}, \dot{Q}_{Y\text{in}}, \dot{Q}_{Z\text{in}}$ are the heat transfer rates into the control volume along the x, y, and z axes, respectively.
- $\dot{Q}_{X\text{out}}, \dot{Q}_{Y\text{out}}, \dot{Q}_{Z\text{out}}$ are the heat transfer rates out of the control volume along the x, y, and z axes, respectively.

The heat transfer mechanism on each side of the block will be determined by the type of material of the neighboring blocks. If the neighboring block would be a solid material, conductive heat transfer will be applied and if it would be a fluid or gas convective heat transfer. Radiative heat losses are not included in this equation since inserting these losses into the equation will make it quadratic which over complicates the calculation. Instead, the radiative heat losses are included in a separate 1D heat transfer model for the top losses of the collector that will be further explained in section 3.3.

The new temperature of each block will be calculated after a given timestep in the unsteady case and after an iteration in the steady case. In order to do that, a rewritten form of Equation 3.1 where only the future temperature of the block remains on the left side of the equation will be filled in with the corresponding heat transfer mechanisms. The model determines the correct heat transfer mechanism by looking at the thermal conductivity coefficient and use the proper corresponding equation. This means that for each possible combination of bordering convective heat transfer and bordering anisotropic conductive heat transfer a unique equation is required. A selection of those equations for all the cases are further explained next.

3.1 Unsteady state heat transfer

In the unsteady heat transfer case, all calculations are time dependent. Every calculated temperature will be the next temperature after a given timestep. With assigned starting values, a causal simulation can be performed that can be used for daily simulations or longer time periods. The rewritten form of Equation 3.1 when performing isotropic conduction on all sides looks as follows:

Isotropic conduction:

$$\begin{aligned} T(y,x,z)^{n+1} =& \beta(y,x,z) \cdot T(y,x,z) \\ &+ Fo_X(y,x,z) \cdot (T(y,x+1,z) + T(y,x-1,z)) \\ &+ Fo_Y(y,x,z) \cdot (T(y+1,x,z) + T(y-1,x,z)) \\ &+ Fo_Z(y,x,z) \cdot (T(y,x,z+1) + T(y,x,z-1)) \end{aligned} \tag{3.2}$$

In the rewritten form of the function a beta factor and different Fourier numbers can be seen. The detailed calculations of these factors can be seen in detail in Appendix A but remain as factors here for brevity. The beta factor usually hovers between zero and one and plays an important role in the determination of the stability of the model. If this factor would fall below zero it would mean that the system is unstable and will diverge to infinity. The factors that play a key role in this would be the chosen resolution of the of the blocks in the X,Y and Z dimension and the size of the timestep. Smaller resolutions would require a smaller timestep and vice versa.

The Fourier numbers would be direction dependent if the resolution dimensions dx,dy and dz would differ from each other. For the chosen design that consists of mostly flat plates and thin walls in certain direction, the freedom to choose these dimensions independently is encouraged. All non-temperature factors in the equations are dependent on the material and need to be calculated for each material that is used respectively.

Single border conduction:

$$\begin{aligned} T(y,x,z)^{n+1} =& \gamma_X(y,x,z) \cdot T(y,x,z) \\ &+ 2 \cdot Fo_X(y,x,z) \cdot (Bi_X(y,x,z) \cdot T(y,x+1,z) + T(y,x-1,z)) \\ &+ Fo_Y(y,x,z) \cdot (T(y+1,x,z) + T(y-1,x,z)) \\ &+ Fo_Z(y,x,z) \cdot (T(y,x,z+1) + T(y,x,z-1)) \end{aligned} \tag{3.3}$$

In this formula, the condition is that one neighboring block on the 'X' side consists of either a fluid or gas. the formula requires a gamma factor before the current temperature and the Biot number for the temperature in the direction of the convective boundary. The calculation of this new gamma factor can again be seen in Appendix A with in addition more for double border and triple border convection. The gamma factor must also stay above zero for model stability. If the block would have two or three borders, the multiplication by two with the terms on the respective axis and the multiplication of the Biot number with the corresponding temperature of the convective side should be added.

While the unsteady heat transfer approach may lead to the most realistic outcomes, because all used factors are both dependent on the material and the direction numerous calculations must be performed before the heat transfer calculations. This may lead to lengthy scripts and long calculation times. Therefore another approach where the steady state of the module is calculated is also performed.

3.2 Steady state heat transfer

In contrast to the unsteady state approach the steady state approach is time independent and material independent for anisotropic conduction. Instead the steady state approach calculates the respective temperatures of all blocks in the module where the sum of all the heat transfers would be zero and undergoes a given amount of iterations through the calculations. This saves the calculations of many factors and also saves calculation time. A condition would be that the model would only interpolate the temperatures within given boundary conditions to a temperature distribution so every node in the matrix of the module will fall under the interpolation unless the original temperature is reassigned to the respective node after each iteration. Time dependent equations can also not be added to the steady state equations. The steady state approach for isotropic conduction is given below:

$$\begin{aligned} T(y,x,z)^{n+1} = &\left(\frac{1}{\frac{2}{dx^2}+\frac{2}{dy^2}+\frac{2}{dz^2}}\right)\cdot \\ &\left(\frac{T(y,x+1,z)+T(y,x-1,z)}{dx^2}+\frac{T(y+1,x,z)+T(y-1,x,z)}{dy^2}\right. \\ &\left.+\frac{T(y,x,z+1)+T(y,x,z-1)}{dz^2}\right) \end{aligned} \tag{3.4}$$

In here no factor nor material properties are present. It only requires the current temperature of the selected block and its neighbouring blocks with their dimensions. Because most blocks in the module matrix fall under this equation, calculation can be done much faster when compared to unsteady state conduction. In case one neighbouring block would consist of another material, a different approach must be used. The temperature on the boundary has to be calculated while following the Dirichlet boundary condition. This means that the heat transfer on the boundary must be equal when approached from both sides. The resulting boundary temperature will be as follows:

$$Tb_X(y,x,z) = \frac{k(y,x,z)\cdot T(y,x,z)+k(y,x+1,z)\cdot T(y,x+1,z)}{k(y,x,z)\cdot k(y,x+1,z)} \tag{3.5}$$

For calculation on material boundaries, the material properties are needed but only the thermal conductivity coefficient. Inserting the boundary temperature with the respective dimensions of the block the new temperature equation will be the following:

$$\begin{aligned} T(y,x,z)^{n+1} = &\left(\frac{1}{\frac{3}{dx^2}+\frac{2}{dy^2}+\frac{2}{dz^2}}\right)\cdot \\ &\left(\frac{2\cdot Tb_X(y,x,z)+T(y,x-1,z)}{dx^2}+\frac{T(y+1,x,z)+T(y-1,x,z)}{dy^2}\right. \\ &\left.+\frac{T(y,x,z+1)+T(y,x,z-1)}{dz^2}\right) \end{aligned} \tag{3.6}$$

The change in parameters are due to the fact that now only half the thickness must be used from the block since the other half is from the other material. More variations like multiple boundaries or single block layers are shown in Appendix A.

The convective boundary conditions in the steady state approach only require the convective heat transfer coefficient (hc) and the thermal conductivity coefficient. The convective heat transfer

coefficient is influenced by the shape of the module and the surrounding medium and thus needs to be calculated separately. In this research, a limited selection of empirical formulas are used for the convective heat transfers to the fluid in the pipes and the convective heat transfer on the top of the module. The convective heat transfer to the pipes is treated to be forced convection in a fully developed flow in a tube which uses a constant Nusselt (Nu) number of 4.36. The convective losses on the bottom and sides of the module are neglected which is similarly done by (Zondag (2002)). To include convective heat transfer as a boundary condition for the pipe walls, additional equations are needed for all possible combinations of pipe wall material neighboring a fluid. For the steady state temperature equation respecting convection on one side on the X axis is the following:

$$\begin{aligned} T(y,x,z)^{n+1} =& k(y,x,z) \cdot \left(\frac{1}{\left(\frac{1}{dx^2} + \frac{1}{dy^2} + \frac{1}{dz^2}\right) \cdot k(y,x,z) + \frac{hc}{dx}} \right) \cdot \\ & \left(\frac{hc \cdot T(y,x+1,z)}{dx} + \frac{T(y,x-1,z)}{dx^2} + \right. \\ & \left. \frac{T(y+1,x,z) + T(y-1,x,z)}{2 \cdot dy^2} + \frac{T(y,x,z+1) + T(y,x,z-1)}{2 \cdot dz^2} \right) \end{aligned} \tag{3.7}$$

As like the previous equations, more combinations can be found in Appendix A. The equations from section 3.2 are used on the bottom side of the collector under the PV material. All the layers on top of the PV and the PV layer itself are thin plates. In addition, since radiative heat losses from the top are a principal loss mechanism in PV modules these cannot be omitted from the model even though they cannot be easily implemented into the FEM model. As a solution, the losses on top of the PV material are treated as a 1D thermal heat transfer mechanism. This approach will be treated in the next section.

3.3 Collector top losses

The heat transfer mechanism equations are empirically determined natural convective equations and radiative heat transfer equations. The collector in this situation would be a glazed flat plate with an inclination and gray-body radiative heat transfer to the environment. It is assumed that heat transfer to and from the sides is neglected. These equations represent all the energy received and emitted by the topglass so the sum of all four heat transfer rates should be zero. With using the energy conservation principle the topglass temperature can be calculated. The equations are the same that were used in (Zondag (2002)). The choice of using these calculations is made because the results of this model will be compared to those of the mentioned research and its measured values for validation. The heat transfer equations are stated below:

$$Q_{air,rad} = A_{PV} \cdot \frac{\varepsilon_{topglass} \cdot \varepsilon_{lam}}{\varepsilon_{topglass} + \varepsilon_{lam} - \varepsilon_{topglass} \cdot \varepsilon_{lam}} \cdot \sigma \cdot (T_{lam}^4 - T_{topglass}^4) \tag{3.8}$$

$$Q_{air,conv} = A_{PV} \cdot \frac{Nu_{air} \cdot k_{material}}{L_c} \cdot (T_{topglass} - T_{ambient}) \tag{3.9}$$

$$Q_{sky,rad} = A_{PV} \cdot \varepsilon_{topglass} \cdot \sigma \cdot (T_{topglass}^4 - T_{sky}^4) \tag{3.10}$$

$$Q_{sky,conv} = A_{PV} \cdot \frac{Nu_{wind} \cdot k_{material}}{L_c} \cdot (T_{topglass} - T_{ambient}) \tag{3.11}$$

Equation 3.8 calculates the radiative heat transfer from the PV laminate to the topglass of the module. ε_{lam} would be the emissivity of the PV laminate and $\varepsilon_{topglass}$ that of the glass cover above the air gap. The Nusselt numbers are from (Fujii and Imura (1972)) for the convective heat transfer from the topglass to the environment and (Duffie and Beckman (2013)) for the convective heat transfer from the PV module to the topglass. For the convective equations the direction of heat transfer can only be from the PV module to the topglass and from the topglass to the environment. In the case of an ambient temperature higher than the topglass temperature other empirical equations for the Nusselt number are required. For this research, in the situation where the ambient temperature would be higher than the topglass, it is assumed that the thermal collector is shut off.

3.4 Performance calculations

When the operation temperature of the PVT collector is calculated with the heat transfer equations the electrical and thermal performance and efficiencies of the PVT collector can now be achieved. These will help indicate if a certain collector archetype or changed design parameter will either improve or worsen the performance. The performances and efficiencies will also be the measure to validate if the model gives realistic results by visualizing them as a function of reduced temperature (T_{red}). This temperature can be visualized as:

$$T_{red} = \frac{(T_i - T_a)}{G} \tag{3.12}$$

T_i represents the inflow temperature of the heat extraction medium, T_a the ambient temperature of the environment and G the effective irradiation on the collector. This form of visualization is used to determine the performance of a PVT collector due to the linear dependency of the efficiencies on the reduced temperature. This way, the performance of the PVT collector can be validated easily by checking if the slopes and values of the linear curves of the resulting efficiencies from the simulation and the measured efficiencies coincide.

Electrical performance
The electrical performance of the PV module that is both dependent on irradiance as well as module temperature is approached by calculating the operation voltage and current using the module parameters and the data results from the model. The equations are used from (Smets and et al (2016)). The irradiance dependency of the outgoing voltage can be expressed as followed:

$$V = Voc + N_{\text{cells}} \cdot k_{\text{b}} \cdot T_{\text{STC}} \cdot \left(\log \left(\frac{I}{G_{\text{STC}}} \right) \right) \tag{3.13}$$

The outgoing current with its dependency on irradiance is expressed as shown below:

$$I = Isc \cdot \left(\frac{I}{G_{\text{STC}}} \right) \tag{3.14}$$

The resulting efficiency that can then be calculated using the previous formulas and an additional expression for the dependency on temperature would be the following:

$$\eta_{\text{el}} = \left(\frac{I \cdot V \cdot FF}{I \cdot A} \right) \cdot (1 + k_{\nu} \cdot (T_{\text{module}} - T_{\text{STC}})) \tag{3.15}$$

The power output would then be calculated as followed:

$$P = \eta_{\text{el}} \cdot (I \cdot A) \tag{3.16}$$

The first two formulas for the voltage and current are only based on irradiance dependency. The electrical efficiency formula adds the thermal dependency of the PV material. Any PV module can be used for these calculations as long as their parameters are known. Further factors that influence electrical performance like degradation, shading and dust collection are not taken into account in the electrical performance calculations.

Thermal performance
The thermal performance and efficiency is calculated by using the resulting heat transfer from the PV material to the bottom calculated by the FEM model (Q_{water}). This is done by summing up the heat transfer in all directions except to the bottom for every PV material point that borders to another material. To give additional insight to the thermal performance the outflow temperature of the heat extraction medium calculated as well. The formula for the outflow temperature of the heat extraction fluid would be as shown below:

$$T_{\text{outflow}} = \frac{Q_{\text{water}}}{C_{\text{fluid}} \cdot \dot{m}} + T_{\text{inflow}} \tag{3.17}$$

The formula for the efficiency would be the outgoing heat rate divided by the incoming energy rate from solar irradiance:

$$\eta_{\text{th}} = \frac{Q_{\text{water}}}{I \cdot A} \tag{3.18}$$

Model execution of calculating PVT collector performance
Now with all the heat transfer and performance equations derived everything can be combined to calculate the electrical and thermal performance of the PVT collector for daily simulations, yearly simulations or reduced temperature efficiency calculations. The approach of the framework model on how it will calculate the correct result and what input data it needs will be explained below.

1. **Input data**
   All what the model would need for the performance calculations are weather data, PV module parameters and module design dimensions. The weather data would only consist of irradiance and ambient temperature in form of a vector in this research. Wind speed is assumed to be always 1 m/s because the reference research of (Zondag (2002)) uses only normal convection with a fixed wind speed in their calculations. The vectors could be given in any preferred time resolution but it is used on an hourly basis in this research. The design of the collector has to be given as a 3D matrix with the starting temperatures and a 3D matrix containing the thermal conductivity coefficients of the materials used in their respective place. In this research the 3D matrices are mathematically determined and automated so that it would change accordingly when design parameters are changed like the number of pipes and pipe thicknesses. When other more complex designs are implemented it would not be any different for the heat transfer equations since the matrix consists out of the same blocks but it would be more of a challenge to mathematically draw it in a 3D matrix. More about this topic will be discussed in chapter 6.

2. **Heat transfer calculations**
   When all the required input data is given the model will calculate the heat losses transferred to the top of the PVT module. It will begin using a predetermined PV operation temperature as a boundary temperature and will find the topglass temperature where conservation of energy applies. Next it will use the same PV operation temperature as a boundary temperature for the FEM numerical model on the bottom and it will calculate the new temperature of every material point using the their respective equations. It will recalculate the new temperature for every point a predetermined n amount of times.

3. **Finding PV operation temperature**
   If the model is finished with the heat transfer calculations it will divide all the calculated energy that has come into the system with what has gone out of the system. If the resulting number does not fall within an error of 1% from equality it will change the PV operation temperature accordingly with by small step. This process is repeated until the error falls within the error margin of 1%.

4. **Output data**
   When the proper PV operation temperature is found it will be used in the thermal and electrical performance calculations. The results of these calculations will be put in a vector with the same length as the weather data vectors and the process will begin again at step 2 for the next hour in the vector. The model will run until all values of the vector are filled in. The results will be the electrical and thermal efficiency, the fluid outflow temperature, the PV operation temperature, the electrical power generated, the thermal power collected and the losses of the system.

3.5 Assumptions

- **All heat transfer equations used are linear**
  To simplify the simulation all heat transfer equations are linear in combination with the numerical approach of the model. Otherwise the model would require geometrically specific equations which takes away the flexibility of the model.

- **The system is treated to be in steady state**
  As previously mentioned, if the unsteady state approach would be used the calculation time would be lengthened by a great margin by the small time step needed to perform a stable simulation. A steady state approach omits this limitation.

- **Convective losses to the bottom and sides of the module are neglected**
  Since the module is thin the losses to the side would be negligible. In addition, because the module is fairly insulated at the bottom the losses in the bottom of the module are neglected as well. The same is done in (Zondag (2002)).

- **The heat transfer to the bends in the design is neglected**
  The smallest resolution possible for the blocks in any dimension is limited by the smallest material thickness in that respective dimension, for this design that would be the pipe thickness. The middle section forms the largest part of the PVT module. If only that section would be needed the resolution in the depth of the module could be set fairly large in order to get less data points that have to be calculated. When the bends are taken into account the resolution in the depth has to be set as small as the resolution of the other two cross-section dimensions. A separate section with a bend was used to determine the heat transfer and it was much smaller than that of the middle section so it is therefore omitted in the model for shorter calculation time.

- **Only normal convection from PV to topglass and topglass to ambient is used**
  The direction of convective heat transfer from the top is treated to be from the PV material to the topglass and from the topglass to the environment. In case the direction should be reversed, the convective heat transfer to the environment is set to zero. This is done because in that situation other heat transfer equations would be needed to determine the proper heat transfer to the module. A further explanation is given in chapter 6.

- **Windspeed is always set 1 m/s for the heat transfer equations**
  Because the used reference validation research of (Zondag (2002)) only measures natural convection where wind speeds are always set to 1 m/s and are further not used in the convective heat transfer equations it is also assumed that the wind speed would 1 m/s in this research.

- **If the irradiance falls below 100 W/m^2 the PVT collector is regarded as off in the model**
  The model used for the performance calculation uses the energy conservation principle to determine the operational temperature of the PV module. The outgoing energy must be equal to the incoming energy and that equality is iteratively found by the model within an error margin of 1 %. At irradiances below 100 W/m^2, small changes in PV module temperature will give larger deviations in errors and increases the calculation time of the model. While the PV part of the PVT collector would normally still produce electricity, because those contributions of irradiances below 100 W/m^2 play a small part to the daily overall performance it is therefore neglected.

- **The inflow fluid temperature in the pipes is used as a uniform boundary temperature for the numerical model**
  Because the fluid temperature in the pipe is dependent on the heat gained from the collector and the heat transfer rate is dependent on the fluid temperature along the pipe, the results from one simulation has to be fed back into the model with the newly calculated fluid temperatures as a boundary condition and this has to be repeated until an equilibrium has been found. Since iteratively finding this equilibrium would lengthen the calculation time of the model severely the fluid temperature is treated to remain the inflow temperature in the numerical model and the resulting heat transfer to the bottom would be multiplied by a correction factor of 0.8 to counter getting higher efficiencies than normal. The value of this factor is determined by measuring the difference between outflow temperatures from a simulation result of the model without a correction factor and measured outflow temperatures from (Zondag (2002)).

3.6 Conclusion

The goal of this chapter was to define the heat transfer equations necessary for the thermal and electrical performance calculations of the previously selected PVT reference collector for validation with measured empirical data. By using a FEM approach for the calculation of the heat transfer to the bottom of the collector and 1D heat transfer equations used in (Zondag (2002)) for the calculation of the losses through the top of the collector the thermal and electrical performance can now be calculated. The resulting efficiencies will be visualized as a function of reduced temperature for easy validation. Assumptions have been made to reduce calculation time. Important assumptions are the steady state approach for the calculation of the FEM model, the omission of the wind speed variation, the uniform fluid boundary temperature and the resulting correction factor of 0.8 that is used to rectify differences in efficiencies.

Chapter 4

Model validation and sensitivity analysis

This chapter will validate the simulation output of the model used with empirical measured data. In addition it will also present a sensitivity analysis with simulation results where different design parameters and dimensions are used. These results compared to the measured values of the reference archetype can give insight in performance behaviour and can be further explored in optimization research. In this research it will be used as a sensitivity analysis for further validation of the model.

4.1 Initial properties

As part of the input data needed, the module specifications used in the validation of the model are stated in Table 4.2. The PV module used in this research should be the same PV module used in (Zondag (2002)), however not all data needed for the simulation was provided by the reference research and a datasheet was not included. Only the Standard Test Conditions efficiency of 11% and temperature coefficient of -0.0045 $^oK^{-1}$ were given, therefore the Voc, Isc, number of cells and Fill Factor were used from a different module. The used model in this research is the Duomax Plus monocrystalline silicon solar module from TrinaSolar (TrinaSolar (2017)). The number of cells and the Voc is reduced to get the original efficiency of 11% from Zondag (2002). The resulting input module variables are stated below. The number of cells and the Voc are adjusted so that all module areas are equal and the STC electrical efficiencies are that of their respective module.

Table 4.1: Module Specifications for the TrinaSolar module (TrinaSolar (2017))

Parameter	**Value**
STC Irradiance (G_{STC})	1000 W/m^2
STC Temperature (T_{STC})	25°C
Number of Cells (N_{cells})	40
Temperature Coefficient (k_ν)	-0.0039 °K^{-1}
Open-Circuit Voltage (V_{oc})	26.389 V
Short-Circuit Current (I_{sc})	9.71 A
Fill Factor (FF)	0.81
Boltzmann Constant (k_{b})	8.61×10^{-5} eV/K

Table 4.2: Module Specifications for the reference PVT collector

Parameter	**Value**
STC Irradiance (G_{STC})	1000 W/m^2
STC Temperature (T_{STC})	25°C
Number of Cells (N_{cells})	40
Temperature Coefficient (k_ν)	-0.0045 °K^{-1}
Open-Circuit Voltage (V_{oc})	15.22 V
Short-Circuit Current (I_{sc})	9.71 A
Fill Factor (FF)	0.81
Boltzmann Constant (k_{b})	8.61×10^{-5} eV/K

For the whole collector design, material properties are also needed. In (Zondag (2002)), bulk layers were made of multiple materials with a mean of the material properties. In this research

each individual material has its respective material properties. Table 4.3 lists the thermal conductivity, density, and specific heat of various materials used in the PVT module. This includes copper, aluminium, PV semiconductor material, EVA top layer, TED layer, adhesive, glass (PV), insulation, fluid, and air.

Table 4.3: Material Properties for the PVT collector

Material	**Thermal Conductivity** (W/mK)	**Density** (kg/m^3)	**Specific Heat** (J/kgK)
Copper	389	8900	386
Aluminium	237	2702	880
PV Material	148	2330	760
EVA Top Layer	0.23	921	2300
TED Layer	0.15	1200	1250
Adhesive	0.16	1200	1250
Glass (PV)	1.1	2200	670
Insulation	0.034	20	670
Fluid	0.6	998	4182
Air	0.0261	1.220	1007

4.2 Validation and sensitivity Analysis

With the initial propertiesm the model validation and sensitivity analysis can be performed. To see if the the PVT collector in the simulation behaves the same as the measured module of the reference research the reduced thermal efficiency curve introduced in Equation 3.12 is used. This curve gives a clear representation on how the collector operates under different ambient temperatures, inflow temperatures and irradiances. The simulation will be performed with a varying irradiance and the results will be visualized next to the measured efficiencies from (Zondag (2002)). Sequentially, various design parameters, dimensions and materials will be changed for the sensitivity analysis. Table 4.4 outlines key parameters such as water flow rate, pipe dimensions, insulation thickness, and environmental conditions.

Table 4.4: Sensitivity analysis range

Parameter	**Base value**	**Range**
Water Flow Rate ($\dot{m}$)	0.02 kg/s	-
Pipe Spacing	0.095 m	-
Insulation Thickness	0.02 m	-
Irradiation (I)	800 W/m^2	[300 W/m^2 - 800 W/m^2]
Sky Temperature	4°C	-
Ambient Temperature	20°C	-
Different Conduction Materials	Cu/Al	[Cu/Al Al/Al Al/Cu Cu/Cu]
PV module	Reference module	[TrinaSolar JinkoSolar SunPower]
Number of Pipes	15	[5 10 15 20 25]
Pipe Wall Thickness (mm)	4	[3 4 5]
Inclination angle (degrees)	45	[0 20 45 60]
Pipe radius (mm)	5	[5 10 20]

The base values are stated in the middle which are the same values used in the reference case. The varying parameters are stated in the right. Every simulation one of the parameters will change while the rest remain the base value. The simulations will run for irradiances ranging from 300 W/m^2 to 800 W/m^2 in steps of 100 W/m^2. The type of PV module will also be changed to see how new commercial modules perform with the same thermal collector. The parameters of one of those modules is stated in Table 4.1, other monocrystalline PV modules

are the CheetahPerc from JinkoSolar (JinkoSolar (2017)) in Table 4.5 and the SunPower X series from SunPower (SunPower (2016)) in Table 4.6.

Table 4.5: Module Specifications for the JinkoSolar module JinkoSolar (2017)

Parameter	**Value**
STC Irradiance (G_{STC})	1000 W/m^2
STC Temperature (T_{STC})	25°C
Number of Cells (N_{cells})	40
Temperature Coefficient (k_ν)	-0.0037 °K^{-1}
Open-Circuit Voltage (V_{oc})	27.667 V
Short-Circuit Current (I_{sc})	10.36 A
Fill Factor (FF)	0.78
Boltzmann Constant (k_{b})	8.61×10^{-5} eV/K

Table 4.6: Module Specifications for the SunPower module SunPower (2016)

Parameter	**Value**
STC Irradiance (G_{STC})	1000 W/m^2
STC Temperature (T_{STC})	25°C
Number of Cells (N_{cells})	68
Temperature Coefficient (k_ν)	-0.0029 °K^{-1}
Open-Circuit Voltage (V_{oc})	48.308 V
Short-Circuit Current (I_{sc})	6.39 A
Fill Factor (FF)	0.79
Boltzmann Constant (k_{b})	8.61×10^{-5} eV/K

4.3 Model validation simulation results

In this section the results from the heat transfer model are presented as a function of the reduced temperature. The reference archetype simulation values will always be represented as a green line for better view.

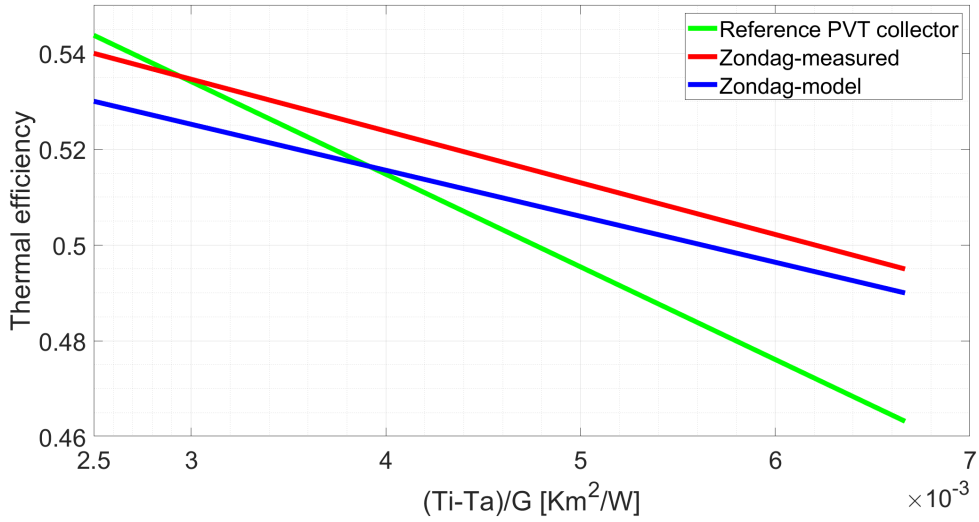

Figure 4.1: Simulation results PVT reference collector

In Figure 4.1 it can be seen that the reference case PVT collector comes close to the measured and simulated values of (Zondag (2002)) but there is a slightly steeper slope in the reference collector case than the measured values. A reason for this might be a higher thermal efficiency change when increasing the PV operation temperature due to assumptions made in deriving the models. Another reason might be the material properties used or the filled in missing values from the original research that are derived from a more recent PV module. By lowering the factor of 0.8 stated in chapter 3 the slope of the line will decrease but also lower the height of the curve overall. In order to adjust the slope of the curve and thus the performance characteristic of the PVT collector there are many factors that can determine the simulation output. If the models are going to be used for further research on PVT optimization which requires results closer to realistic values it would be advised to recreate the PVT collector in an additional measurement set up and revise the measurement results with the simulation results for model calibration.

4.4 Sensitivity simulation results

This section displays the sensitivity simulation results to further validate the performance of the PVT collector. The changed design parameters are stated in Table 4.4 and the resulting figures are stated below:

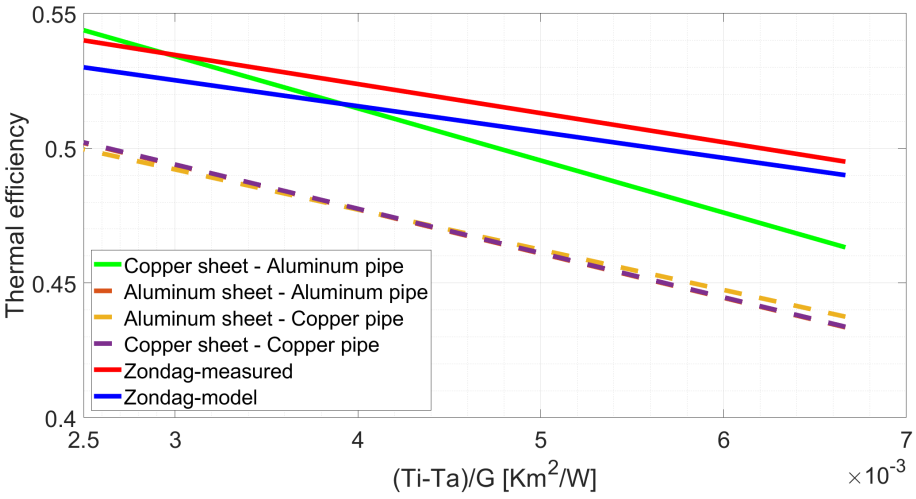

(a) Material experimentation

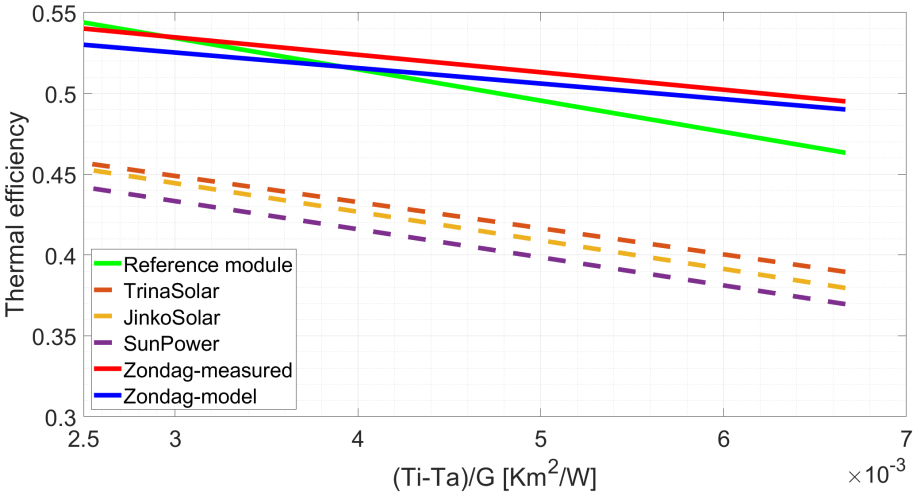

(b) Module experimentation

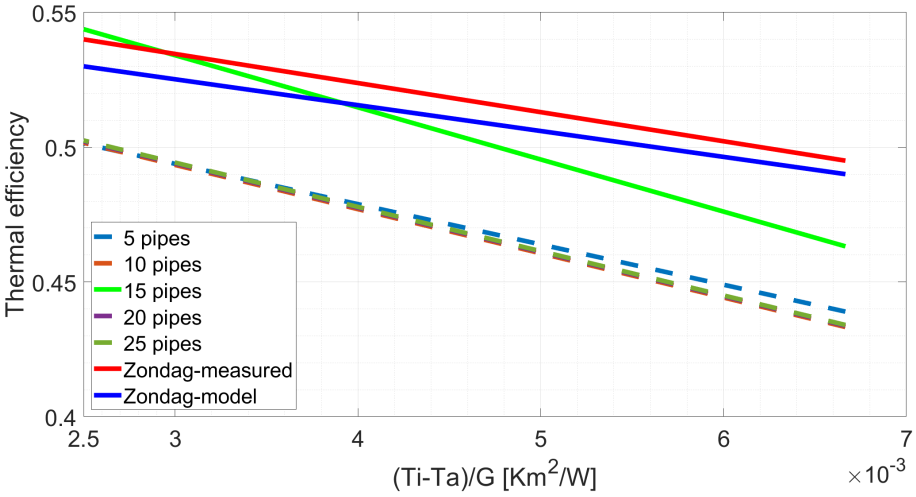

(c) Number of pipe experimentation

Figure 4.2: Experimentation with designs and materials

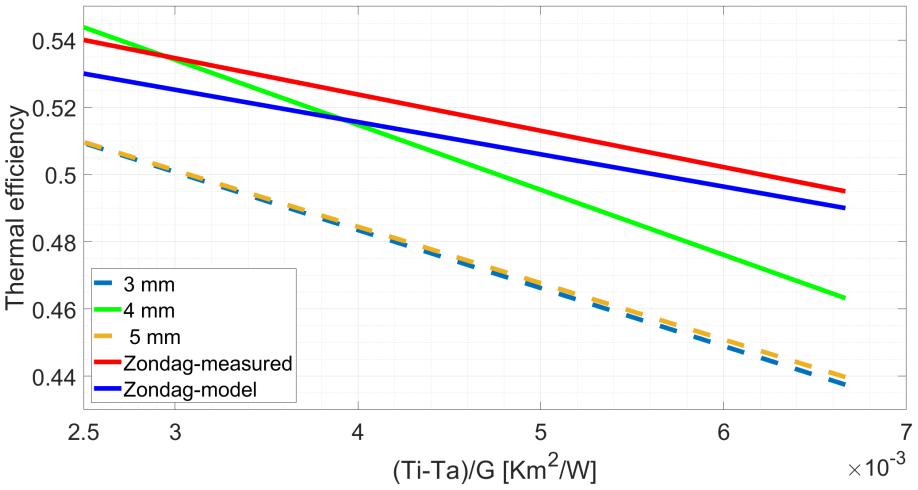

(a) Pipe thickness experimentation

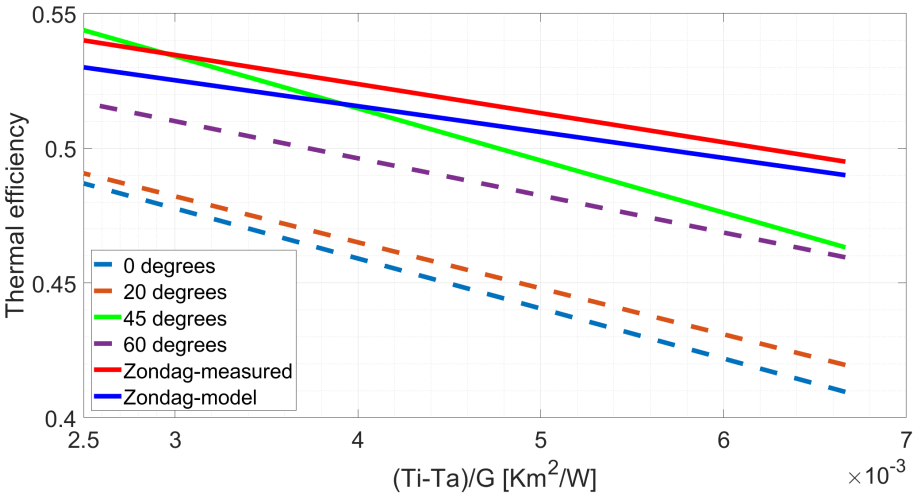

(b) Inclination angle experimentation

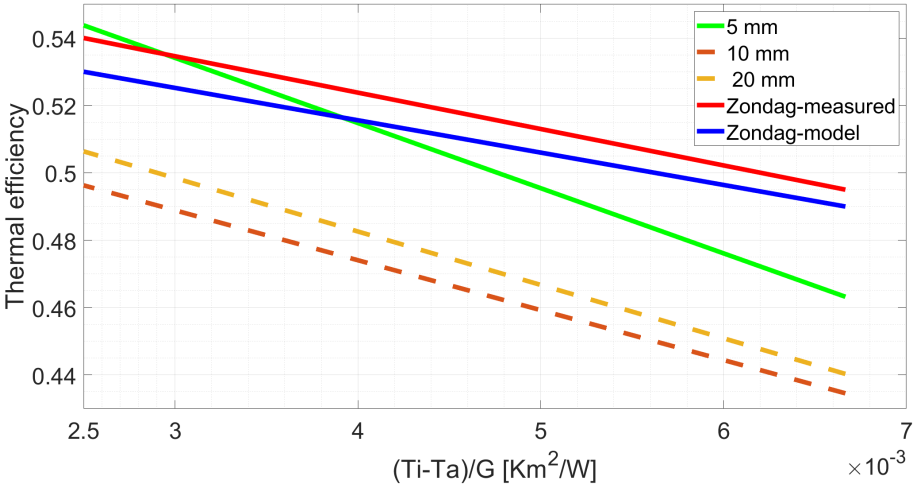

(c) Inner pipe radius experimentation

Figure 4.3: Experimentation with dimensions

In Figure 4.2a it can be seen that the other material combinations appear to give lower efficiencies than the reference collector. This can be due to the change in material properties in the sensitivity simulations that were performed later or in an adjustment in the heat transfer equations. If the conduction to the bottom of the collector would be better in the case of the other material combinations the slope of the curve would be closer to the measured values.

Figure 4.2b gives an overview of the results of using different PV cells instead of the original PV cells used in the reference research. The three modules appear to be lower in thermal efficiency than the reference module. This can be because the electrical efficiency of all the modules are roughly 10% higher than the reference module. More electrical power will be generated which is beneficial for a PVT collector. The SunPower module has the highest STC efficiency and is therefore the lowest in the reduced thermal efficiency curve.

Figure 4.2c shows the the variation in the number of pipes that lie in the collector. More pipes would mean that there is more surface area in the collector for the water to collect heat. Since the archetype has one serpentine pipe and not multiple this does not mean that more water will heat up which would be the case for multiple separate tubes. An optimum appears to be having 15 pipes in the collector.

In Figure 4.3a various pipe wall thicknesses were used in the simulations. Because the pipe wall thickness is the smallest thickness in the numerical model, an increase in thickness would make a numerical jump in the thermal efficiency. A solution to this would be to have a higher resolution in every dimension.

In Figure 4.3b it is presented how the inclination of the module would affect the thermal performance. It can be seen that the higher the inclination angle the higher the thermal efficiency. This would seem counter intuitive since a higher inclination angle would contribute more to the convective losses from the top of the module. I seems that the the losses from the top contribute to better cooling from the top, therefore lowering the operational PV temperature which leads to a higher thermal efficiency even though the output temperature would be lower.

Figure 4.3c gives the results for different pipe radii in the PVT collector. The thermal efficiency stays roughly the same but it must be addressed that a larger pipe radius could transport more water over time with higher mass flow rates. The mass flow rate stays the same in the simulations because otherwise there would be another factor that influences the thermal efficiency.

4.5 Conclusion

The aim of this chapter was to validate the model used in this research with measured data to see if it gives realistic outputs and to perform a sensitivity analysis with different module parameters for further validation. The results show that the model does give values close to the measured values in the research of (Zondag (2002)) while having a steeper slope. It is stated that the values used from other modules that were originally missing in the original research might cause the increase in the slope. The sensitivity analysis shows that the thermal efficiencies are often lower than the reference case. The base values might be an optimum for this module or the conduction to the bottom should be higher in the simulation model.

Chapter 5

Collector performance simulations

In this chapter the aim would be to simulate the PVT collector over various days in the year to see how it will perform in real world conditions. To further validate these performances an economic analysis using LCOE calculation to give additional insights in the yield and costs of a PVT collector is performed. The simulation results will be visualized in form of power distribution curves, efficiency curves and temperature curves. For all the simulations the base values from Table 5.1 are used combined with the the PV module parameters from the SunPower PV module stated in Table 5.2. This module is chosen over the other modules because it has the highest electrical efficiency. The days chosen for the daily simulations are the 2nd days of the months January, May and July. These days are chosen to give an indication on how the PVT collector would perform in the middle of the winter, on a day in spring and in the middle of the summer.

Table 5.1: Base Case Properties for daily simulation

Parameter	**Base value**
Water Flow Rate ($\dot{m}$)	0.02 kg/s
Pipe Spacing	0.095 m
Insulation Thickness	0.02 m
Irradiation (I)	800 W/m^2
Sky Temperature	4°C
Ambient Temperature	20°C
Different Conduction Materials	Cu/Al
PV module	SunPower
Number of Pipes	15
Pipe Wall Thickness (mm)	4
Inclination angle (degrees)	45
Pipe radius (mm)	5

Table 5.2: Module Specifications for the daily simulation module

Parameter	**Value**
STC Irradiance (G_{STC})	1000 W/m^2
STC Temperature (T_{STC})	25°C
Number of Cells (N_{cells})	68
Temperature Coefficient (k_ν)	-0.0029 °K^{-1}
Open-Circuit Voltage (V_{oc})	48.308 V
Short-Circuit Current (I_{sc})	6.39 A
Fill Factor (FF)	0.79
Boltzmann Constant (k_{b})	8.61×10^{-5} eV/K

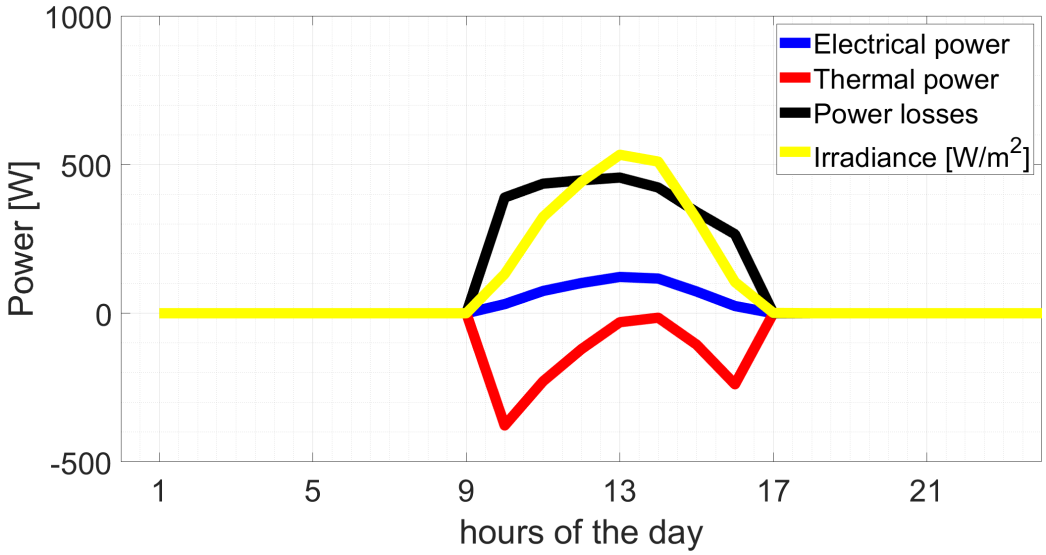

(a) Power distribution January 2nd

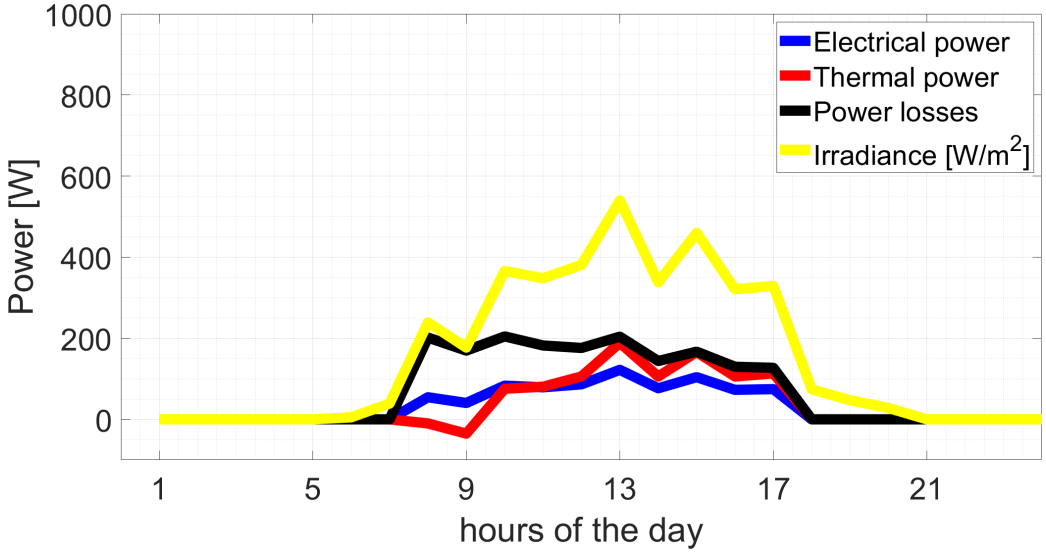

(b) Power distribution May 2nd

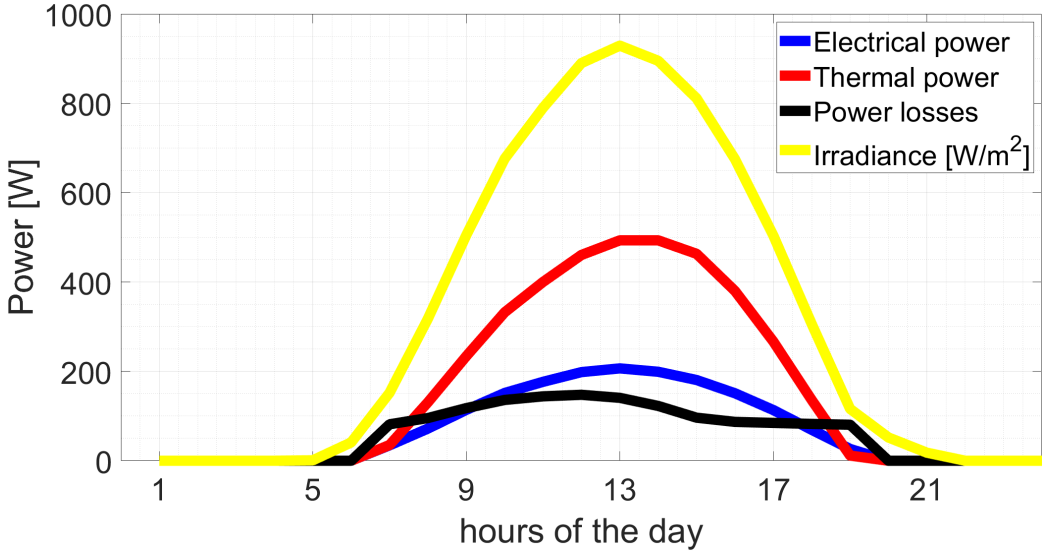

(c) Power distribution July 2nd

Figure 5.1: Power distributions over various days

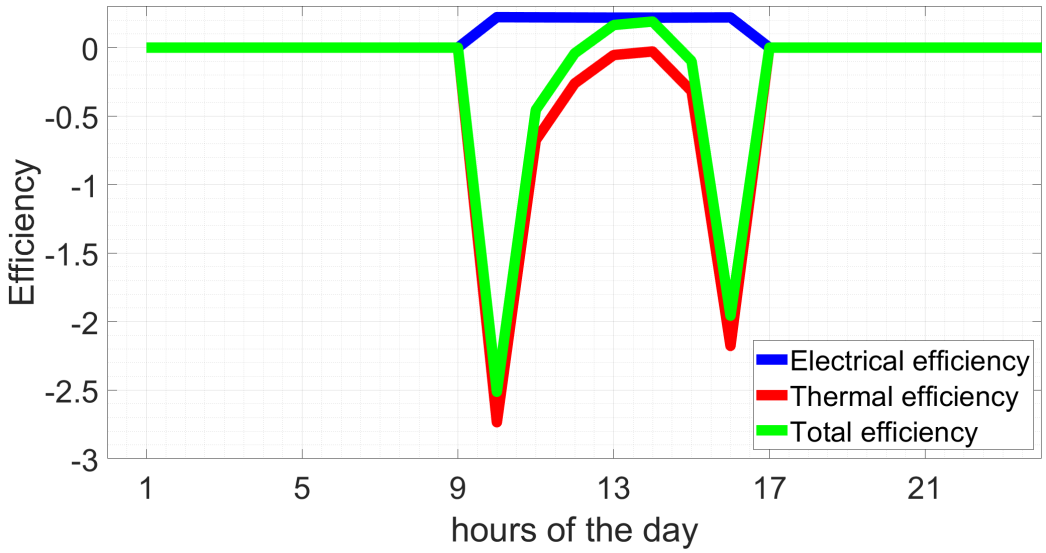

(a) Efficiency distribution January 2nd

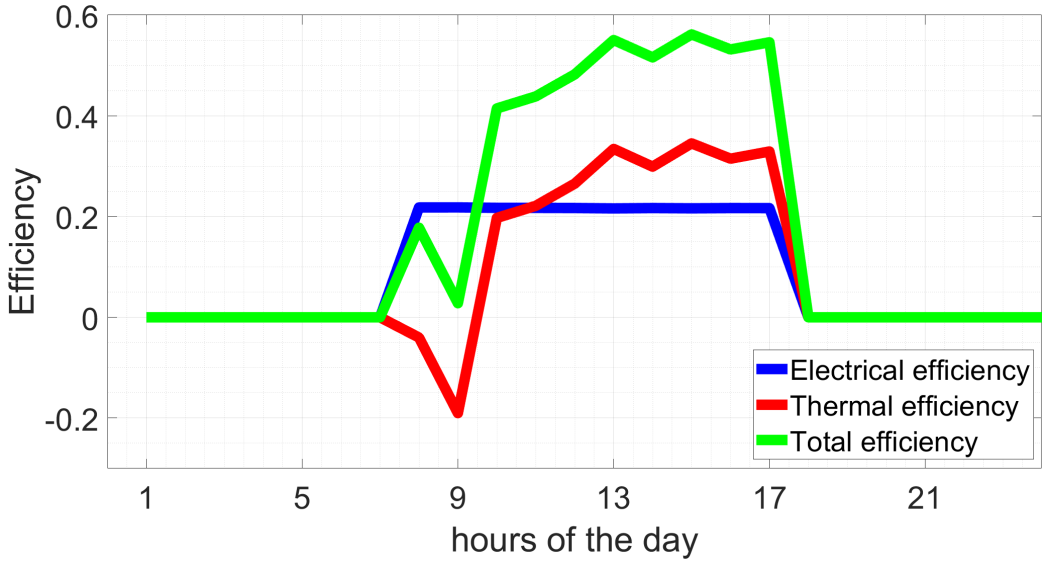

(b) Efficiency distribution May 2nd

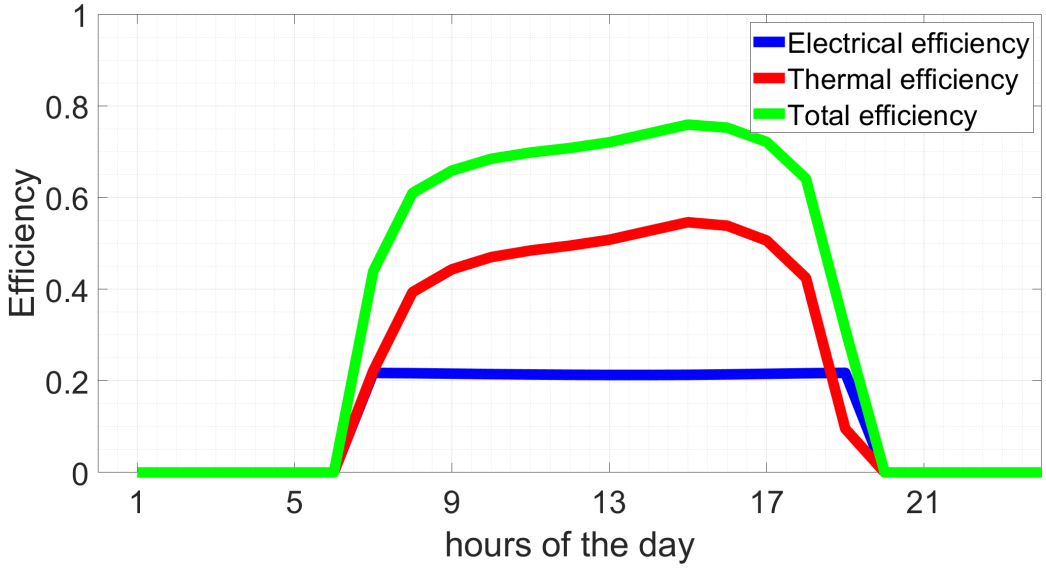

(c) Efficiency distribution July 2nd

Figure 5.2: Efficiency distributions over various days

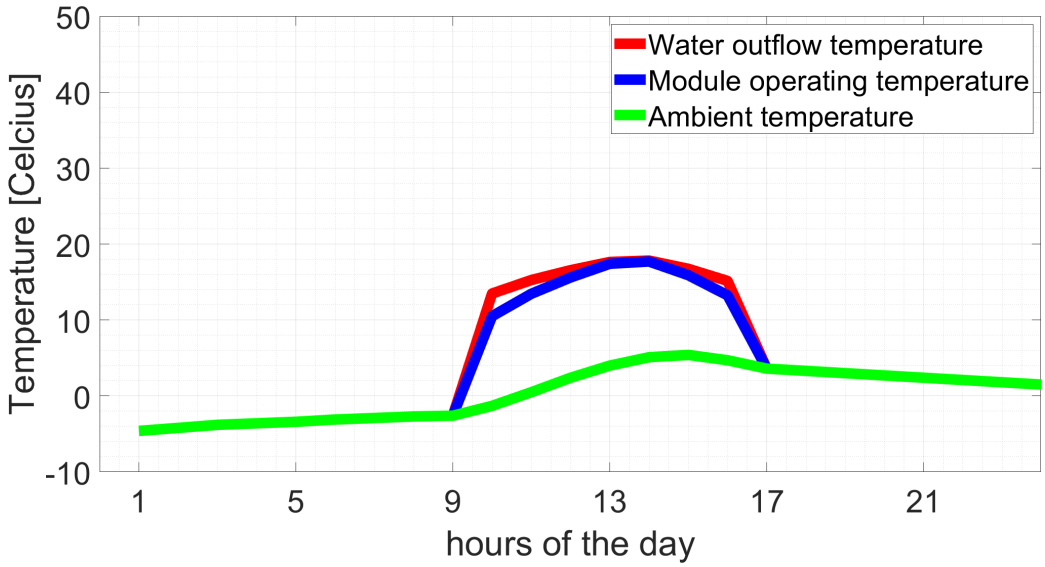

(a) Temperature distribution January 2nd

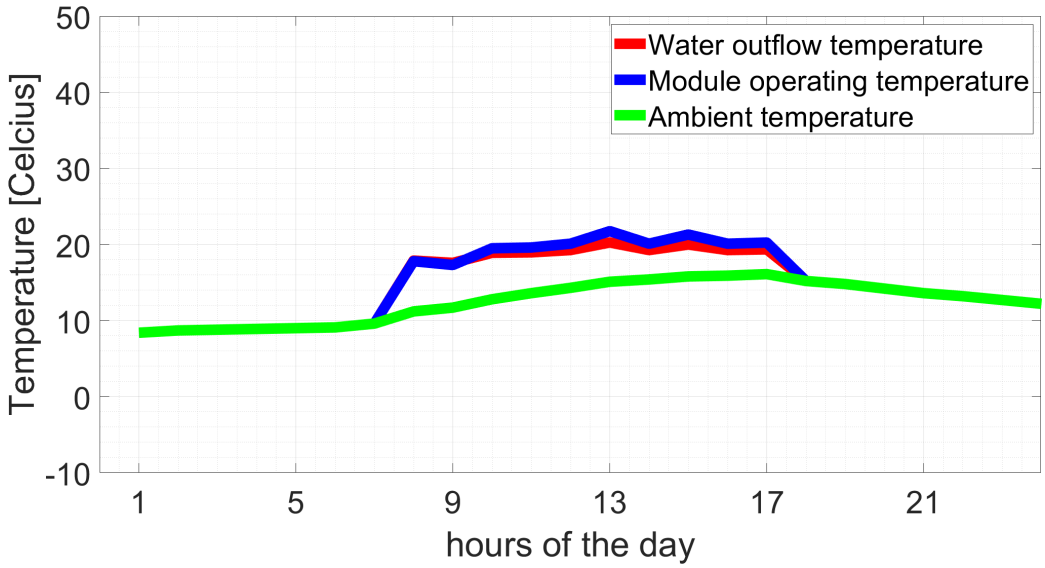

(b) Temperature distribution May 2nd

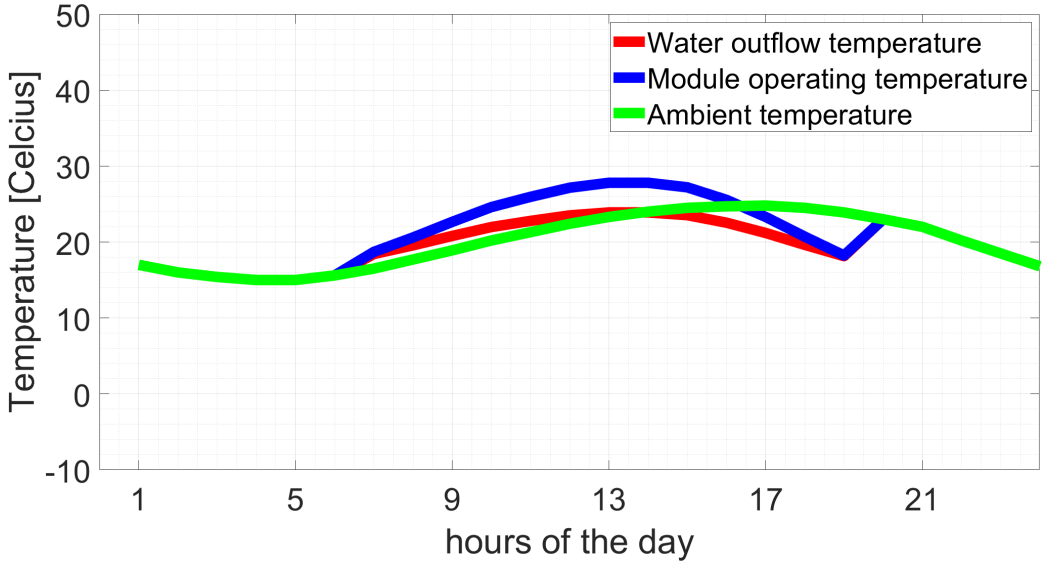

(c) Temperature distribution July 2nd

Figure 5.3: Temperature distributions over various days

5.1 Power

To begin with the power distributions shown in Figure 5.1 it can immediately be seen that the PVT collector loses thermal energy over the day in Figure 5.1a. Because it is a cold day in winter the inflow temperature of 20 ^oC is too high compared to the ambient temperature. This will result in the case that the heat coming from the heat extraction fluid would go through the top instead of gaining heat from the PV cells. It would be more beneficial to have the collector side of the PVT collector turned off. An alternative may be to implement a refrigeration cycle between the PVT collector and the source of the fluid, which would normally be a water storage tank or another storage solution.

Figure 5.1b shows that in spring there are less thermal losses compared to a day in the winter but there are still losses in the morning due to the low ambient temperatures during that time. The solutions to this would be the same here as for the January case but it would be recommended to only have the module turned off during that time instead of implementing a refrigeration cycle. The overall losses are relatively high compared to the incoming irradiance even though the rest of the day there is both thermal and electrical heat gained. I would be more beneficial to install PV modules and Solar thermal modules separately instead of the combined PVT collector when the climate in the region would be more like the spring case.

In Figure 5.1c a more optimal situation can be seen. There is no situation where the inflow temperature would heat up the PV module instead of cooling it off and a peak thermal power of 500 W can be absorbed by the heat extraction fluid. A PVT collector would thus far perform well during hot summers or hot climates.

5.2 Efficiency

Figure 5.2a shows more clearly that a PVT collector does not perform well during the winter or cold climates. Thermal energy almost as much as three times the incoming energy is lost to the environment. A rule of thumb to make sure that no heat would be lost from the inflow when using PVT might be to always have a lower inflow temperature than the ambient temperature.

In Figure 5.2b the efficiencies over the day can be seen as overall good. only in the morning is a slight dip but for the rest of the day the total efficiencies would be between 40 and 60 %. Again, two separate systems of regular PV and solar thermal could be more beneficial to install on spring days.

Figure 5.2c presents high total efficiencies over the day. Record efficiencies for PVT would lay around 80 % so the total efficiency might still be a bit too high. It was said in chapter 4 that the inclination of the thermal efficiency curve was slightly steeper than the reference value. These efficiencies can confirm that there are yet more losses that need to be implemented in the model.

5.3 Temperature

Figure 5.3a illustrates the temperature distribution of the PV operational temperature, the water outflow temperature and the ambient temperature. Because the PVT collector is turned off during time periods with an irradiation below 100 W/m^2 the model sets both the PV operational temperature and the outflow temperature to the ambient temperature. While in reality the PV module cannot be turned off by itself but the circuit can be only opened the real PV temperature would be higher than the ambient temperature. However, since the PV does not contribute electrical power during these times in the model the assumption that the PV temperature would be equal to the ambient temperature should not be a problem.

During the the spring day in Figure 5.3b all the temperatures are closer to each other. From

this figure it is not that visible that there is heat lost to the environment but when looked at closely every time the water outflow temperature would fall below the inflow temperature which is 20 ^oC in this case, heat will be lost.

Figure 5.3c gives a good example of one of the main principles of the PVT collector. After 4 PM it can be seen that the PV operational temperature will be lower than the ambient temperature, yet the figure also indicates that this situation would not occur frequently since only during a hot day in the summer it would be the case on roughly a quarter of the day. If the ambient temperature would be higher, the inflow temperature lower or a combination of both the PVT module would be more beneficial. However in temperate climates it only performs better than conventional PV and solar thermal collectors during the summer.

5.4 Economic analysis

While daily and yearly simulation results of the electrical and thermal performance of a PVT collector give a clear view on its behaviour in terms of energy, to give additional insight on its yield and costs an economic analysis can be made as well. For this, investment costs, operational costs, discount rate and other economic data would be needed. With all this information the LCOE (Levelized Cost of Electricity) can be calculated and compared to with other means of electricity generation like regular PV. The LCOE is calculated by combining the electrical yield and thermal yield of the PVT collector (Dehghan and et al (2024)). The formulas used are stated below:

$$LCOE_{PV} = \frac{C_{PV} + \Sigma_{t=1}^{n} \cdot \frac{C_{O\&M,PV}}{(1+r)^t}}{\Sigma_{t=1}^{n} \cdot \frac{E_{PV}(1-d)^t}{(1+r)^t}} \tag{5.1}$$

$$LCOE_{th} = \frac{C_{th} + \Sigma_{t=1}^{n} \cdot \frac{C_{O\&M,th}}{(1+r)^t}}{\Sigma_{t=1}^{n} \cdot \frac{E_{th}}{(1+r)^t}} \tag{5.2}$$

$$LCOE_{PV+th} = \frac{C_{th} + C_{PV} + \Sigma_{t=1}^{n} \cdot \frac{C_{O\&M,PV+th}}{(1+r)^t}}{\Sigma_{t=1}^{n} \cdot \frac{E_{PV}(1-d)^t + E_{th} \cdot C_f}{(1+r)^t}} \tag{5.3}$$

- C_{PV} and C_{th} denotes investment costs.
- $\Sigma_{t=1}^{n}$ is the representation of the summation of all years.
- $C_{O\&M,PV}$ and $C_{O\&M,th}$ are the Operational and Maintenance expenditures.
- r is the discount rate.
- d is the annual power degradation.
- t is the time step which is a year in this case.
- E_{PV} is the electricity generation in the respective year.
- E_{th} is the thermal energy generation in the respective year.

- n is the financial lifetime of the module
- C_f would be the ratio between the Feed in Tarif (FiT) and the end user costs of electricity supplied by the grid.

Using the electrical and thermal yield generated by the model over the year by the PVT collector, the LCOE can be calculated. In chapter 5 only daily simulations were made on three specific days. Since the model requires much calculation time for the yields of the PVT collector the performance of the PVT on these three days and single days of the other months will be stretched over their respective months during the year in order to replicate a yearly simulation. Figure 5.4 shows the operational PV temperature over the year of the used SunPower PV module alongside a yearly PV only calculation of the other two modules.

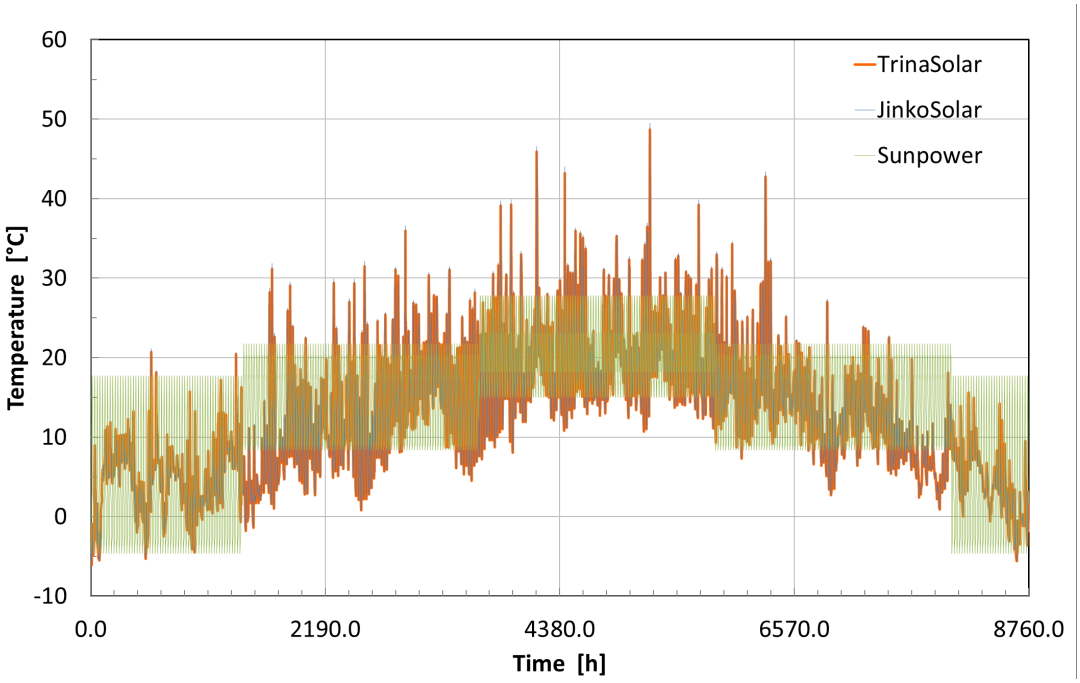

Figure 5.4: Assumption of yearly operation

While the variations are a bit rough during the year the mean operational PV temperatures follow a yearly trend roughly similar to the other PV modules thus the simplification can be used for the calculation of the LCOE. For the costs of a PVT collector data is used from (Dehghan and et al (2024)) and is represented in Table 5.3 which can be seen below:

Table 5.3: Economic data and costs (Dehghan and et al (2024))

Parameter	**Value**	**Description**
C_{PV} \$/module	338	Cost per module
C_{th}	2060	Other system and installation costs
$C_{O\&M,PV}$ \$/kWp	29	Annual O&M costs per installed kWp
$C_{O\&M,th}$ \$/kWp	3.4	Annual O&M costs per installed kWp
E_{PV}	539	Annual electricity yield in year 1
E_{th}	1618	Annual thermal yield in year 1
d %	-1.4	Annual power degradation
N_m yr	25	Lifetime module
r %	2	Discount rate
C_f -	0.5	Ratio between FiT and enduser cost

When putting the data from Table 5.3 in Equation 5.3 the LCOE of the PVT collector would be 0.08 $/kWh over its lifetime. When using the data from the other PV only modules from TrinaSolar and JinkoSolar their LCOE would be around 0.13 $/kWh. The lower LCOE for the PVT is due to the additional thermal energy that can be now utilised that would otherwise be lost to the environment.

5.5 Conclusion

The aim of this chapter was to simulate the PVT collector performance to see how it will perform over the year and in different seasons. In contrast to the reference module used in chapter 4 a more recent PV module was used for the electrical part of the PVT collector. While the PVT collector would perform well during the summer, for days during the spring and during the winter the module could lose thermal energy to the environment making it less beneficial than conventional PV and solar thermal. To give additional insight on the performance of the PVT collector an LCOE calculation is made to give an overview of the yield and costs of a PVT collector. The resulting LCOE was 0.08 $/kWh for PVT and 0.13 $/kWh for standalone PV.

Chapter 6

Discussion

This chapter examines the validity of the performance simulation framework model and performance calculations done in the preceding chapters. It will discuss all the assumptions made and what effect they had on the output and usability of the model. The results of the sensitivity analysis and PVT performance are also addressed.

6.1 Reference collector selection

In chapter 2 a glazed-covered flat plate water cooled PVT collector with serpentine tubes at the back was chosen for the heat transfer equations. The reasons for this were the benefits of the selected archetype, heat extraction fluid and design. A similar collector was used in preceding research done by (Zondag (2002)). This research has performance measurements as well so it would be beneficial to work further on the numerical model made in that research and then test the resulting model with the measured values. The archetype is also commercially used and was more simple to work with for the heat transfer equations.

While the selected archetype was usable in the scope of this research it was not an optimal design by itself. Designs with more contact area can be used as well like web flow absorbers or spiral flow absorbers. Other forms of heat extraction can also be used for better performance of the PVT collector like bifluid based collectors or the combination with phase change materials, heat pumps or refrigerants.

In conclusion, the PVT archetype was useful in the scope of this research and commercially used but it was not an optimal design to use for future PVT archetypes.

6.2 Numerical heat transfer model and assumptions

Chapter 3 presented the approach to calculate the heat transfer inside PVT collector to determine its performances. The numerical approach used the energy conservation principle for every block of material in the design. The simplified approach to calculate the heat transfer in an otherwise complex structure made it possible to calculate heat transfers that otherwise had to be measured first in an experimental setup similarly done in the previous research by (Zondag (2002)). Now that the simulation model was not dependent anymore of a physical setup various designs could be simulated making the model highly flexible.

A problem that arose early in this research was that the calculation time would be a hard limitation on the usability of the model. The unsteady state approach worked but required such small time steps for model stability that a daily simulation would almost take a day to calculate and a yearly simulation was out of the question. The transition to the steady state approach resolved this problem but calculation time would be the reason of many of the other assumptions

that have been made.

Discussion assumptions

Now that the model has become time independent the other contributing factor to the calculation time would be the number of material data points that had to be calculated. In the developed model, it is possible to stretch the resolution in the depth of the collector but the minimal required resolution in the bends forced the model to use a much smaller resolution that was not necessary in the bulk of the collector. The omission of the bends of the serpentine collector resulted in faster calculation times but it made the model less realistic.

The heat transfer direction was set to be only from the PV to the topglass and from the topglass to the environment. This is done because in the previous research these were the only directions that were used. While in that test setup with high inflow temperatures and relatively low ambient temperatures, the occurrence of having a higher ambient temperature than the PV operational temperature was absent. This would not be the case in realistic environments. More heat transfer equations for various situations are therefore needed. In addition, the heat transfer to the environment was set as natural convection only with a set wind speed of 1 m/s. Again, in realistic environments the wind speed can rapidly change changing the type of convection mechanism required.

The heat transfer to the water pipes is determined by calculating the heat transfer to the bottom from the PV material. In the temperature distribution, the water temperature was set to the inflow temperature with a correction factor of 0.8 in order to make the calculation reasonable. This still led to high outflow temperatures and high thermal efficiencies so a more realistic approach is still needed.

6.3 Performance calculations

Due to incomplete input data, assumptions for the PV module were made for the validation of the model. The simulation results were fairly similar to the measured thermal efficiencies in the reference research but there was a slightly higher inclination in the curve of the model used in this research. This may be due to the data assumptions made. When changing different parameters the results did not show much change. Only the inclination angle and the different PV modules used showed forms of different thermal performances.

The daily performance calculations gave more insight in how the PVT collector would operate in different days throughout the year. The results were overall close to realistic performances. These results are more optimistic because of the assumptions stated earlier. The daily simulations show that a PVT collector is usable during summers and hot climates but underperform in colder times and climates. Implementing a refrigeration cycle would make a PVT collector more viable during these periods and climates but that would need additional power to operate.

In conclusion, the PVT archetype sufficed as a reference archetype for the heat transfer calculations but more optimal archetypes could lead to a better PVT performance. The heat transfer models were able to calculate the heat transfer rates without needing an experimental setup but assumptions had to be made to make the calculation times of the model more reasonable making the results less accurate. The performance calculations gave close to realistic values but are a bit more optimistic. Finally, the economic analysis gave insight in the costs of the electrical performance of a PVT collector and concluded that it would be less expensive to use than regular PV.

Chapter 7

Conclusions

This research was done to create a performance simulation framework model that is suitable for the calculation of the thermal and electrical performance for any PVT archetype. This framework model can later be used for PVT collector optimization, archetype experimentation, PVT system integration, environmental PVT performance analysis and economic sustainability research. The overarching goal was structured in four sub-objectives. Each sub-objective will be addressed and answered if that objective has been reached.

- **Sub-objective 1: Choosing a reference collector**
  A glazed-covered flat plate water cooled PVT collector with serpentine tubes at the back was chosen as the reference collector. It was a suitable archetype for the heat transfer equations but more optimal archetypes can be used for higher PVT performances.

- **Sub-objective 2: Formulating the PVT heat transfer calculations**
  Heat transfer equations have been made to calculate the thermal and electrical performance of the archetype PVT module without needing an experimental setup making the model flexible for other archetypes and designs.

- **Sub-objective 3: Validating simulation output**
  The thermal efficiencies resulting from the reference archetype were close to measured values but there was a steeper slope in the curve that was caused by assumptions made in the model.

- **Sub-objective 4: Simulating PVT collector performances**
  The daily performance simulations show that the PVT collector used in this research performs well during hot periods and in hot climates and less in cold periods and climates. The economic analysis shows that the same PVT collector would be cheaper over its lifetime than regular PV.

7.1 Summary of key findings

In this research the primary objective to create a performance simulation framework model has been achieved and has given the following insightful findings:

- **Selected PVT collector**
  This research has visualized that there is a wide variety of PVT archetypes that can be used for current and future generations of PVT collectors. PVT collectors can be combined with heat pumps, refrigeration pumps, phase change materials and multiple forms of heat collection via fluids or air. These combinations can all contribute to high electrical and thermal efficiencies

- **Numerical heat transfer model and assumptions**
  It is possible to calculate heat transfer rates of complex designs when using a Finite Element Method (FEM) approach to calculate the heat transfer within the collector. With the proper convective and radiative equations to the environment, the heat transfer inside the collector and to the environment could be calculated without needing an experimental setup.

- **Performance calculations**
  The performance calculations gave insight into the simulated behavior of the PVT collector when operating in real-world conditions. Ranging the inclination angle from 0 to 60 degrees showed that the thermal efficiency became around 55% at an irradiance of 800 W/m^2 at 45 degrees. It also showed that differences in dimensions like pipe thicknesses and number of pipes did not affect the thermal performance that much. The daily performance calculations illustrated that the thermal energy lost to the environment can be three times as high as the incoming solar energy due to the low ambient temperatures compared to the inflow temperature. In the summer, PVT can achieve high total efficiencies of around 75% making PVT suitable during those times. The economic analysis showed that a PVT collector can have an LCOE of \$0.08/kWh which is lower than the \$0.13/kWh of conventional PV.

7.2 Conclusion and final thoughts

In the prelude of the biggest revolution, the energy revolution, many technologies utilizing renewable energies are needed to achieve a future with net zero carbon dioxide. One of these technologies can be PVT collectors.

When PVT collectors are combined with the proper storage solutions and intermediate systems for optimal performance it may make it possible to sustain households for both electrical and thermal needs making them energy autonomous. These may be small steps but they will bring the world closer the ultimate goal of achieving a sustainable economy globally. Time, money and policies are always the largest constraints when pursuing this goal but every small finding that may bring the end goal closer is worth it. Research by research, thesis by thesis, result by result.

In conclusion, we may be still at the beginning of the energy transition but every part that would make it possible would be useful. PVT technology may not yet be as popular yet than regular PV or solar thermal, it has lots of thermal and electrical potential that is worth investigating.

Chapter 8

Recommendations

The development and analysis of the PVT collector has yielded promising results and insights. However, there remains a significant scope for further refinement and enhancement of the model. The following areas have been identified for future work:

- **Temperature profile of the water inside the pipes:** A key aspect of improving the PVT collector model involves a detailed analysis of the temperature profile of the water flowing through the pipes. This includes assessing the temperature gradients and variations under different operational conditions. A more comprehensive understanding of this profile will enable better predictions of the collector's performance and efficiency.

- **Enhancing the unsteady model for faster calculation times and more realistic results:** The current unsteady model, while effective, can be further optimized for speed and accuracy. The aim is to reduce computational time without compromising the realism of the model. This involves refining the algorithms and possibly integrating more sophisticated numerical methods to simulate the transient behavior of the PVT collector more efficiently.

- **Flow mechanic calculations for realistic convection factors:** Another area of focus is the enhancement of flow mechanic calculations. This includes a thorough analysis of forced convection inside the pipes and the impact of external factors such as wind on convection outside the pipes. Improving the accuracy of these calculations will lead to a more realistic assessment of heat transfer coefficients and overall thermal performance.

- **Implementing a feedback loop that can effectively search for the correct PV operational temperature:** The simulation model finds the correct PV operational temperature by measuring the differences of the incoming and outgoing energy and increases or decreases the PV operational temperature with a small step when they are not equal. This process severely lengthens the calculation time. Additional research can be done to implement a more effective way of finding the right operational PV temperature.

- **Use of different module designs:** Finally, experimenting with various module designs will provide insights into how different configurations affect the performance of the PVT collector. This includes exploring different geometries, material compositions, and layout of photovoltaic cells and thermal components. Comparative analysis of these designs will be instrumental in identifying the most efficient and practical configurations for real-world applications.

Through these enhancements, the PVT collector framework model can be significantly enhanced, leading to more accurate predictions and potentially contributing to the development of more efficient and effective PVT collectors in the future.

References

Abdin, Z. U., and Rachid, A. (2021). A survey on applications of hybrid pv/t panels. *Energies*, *14*, 1201. https://www.mdpi.com/1996-1073/14/4/1205 doi: https://doi.org/10.3390/en14041205

AEE_INTEC. (2021). *Innovative energy technologies in austria - market development 2021.* https://www.aee-intec.at/index.php?params=solarthermiestatistiken-40&lang=en

An, W. (2016). Experimental investigation of a concentrating pv/t collector with cu9s5 nanofluid spectral splitting filter. *Applied Energy*, *184*, 197-206. https://www.sciencedirect.com/science/article/pii/S0306261916314271 doi: https://doi.org/10.1016/j.apenergy.2016.10.004

Awad, M. M. (2022). Performance of bi-fluid pv/thermal collector integrated with phase change material: Experimental assessment. *Solar Energy*, *235*, 50-61. https://www.sciencedirect.com/science/article/pii/S0038092X22001347 doi: https://doi.org/10.1016/j.solener.2022.02.031

Browne, M., and et al. (2015). Phase change materials for photovoltaic thermal management. *Renewable and Sustainable Energy Reviews*, *47*, 762-782. https://www.sciencedirect.com/science/article/pii/S1364032115002038 doi: https://doi.org/10.1016/j.rser.2015.03.050

Bätzner, D. (2011). Properties of high efficiency silicon heterojunction cells. *Energy Procedia*, *8*, 153-159. https://www.sciencedirect.com/science/article/pii/S1876610211016262 (Proceedings of the SiliconPV 2011 Conference (1st International Conference on Crystalline Silicon Photovoltaics)) doi: https://doi.org/10.1016/j.egypro.2011.06.117

Dehghan, M., and et al. (2024). Energy, economic, and environmental analysis of converging air-based photovoltaic-thermal (air/pv-t) systems: A yearly benchmarking. *Journal of Cleaner Production*, *434*, 139871. https://www.sciencedirect.com/science/article/pii/S0959652623040295 doi: https://doi.org/10.1016/j.jclepro.2023.139871

Duffie, J. A., and Beckman, W. A. (2013). *Solar engineering of thermal processes.* John Wiley & Sons.

Dupeyrat, P. (2011). Efficient single glazed flat plate photovoltaic–thermal hybrid collector for domestic hot water system. *Solar Energy*, *85*(7), 1457-1468. https://www.sciencedirect.com/science/article/pii/S0038092X11001125 doi: https://doi.org/10.1016/j.solener.2011.04.002

et al, G. L. (2015). Numerical and experimental study on a pv/t system with static miniature solar concentrator. *Solar Energy*, *120*, 565-574. https://www.sciencedirect.com/science/article/pii/S0038092X1500417X doi: https://doi.org/10.1016/j.solener.2015.07.046

Evola, G., and Marletta, L. (2014). Exergy and thermoeconomic optimization of a water-cooled glazed hybrid photovoltaic/thermal (pvt) collector. *Solar Energy*, *107*, 12-25. https://www.sciencedirect.com/science/article/pii/S0038092X14002813 doi: https://doi.org/10.1016/j.solener.2014.05.041

Fikri, M. A., and et al. (2022). Recent progresses and challenges in cooling techniques of concentrated photovoltaic thermal system: A review with special treatment on phase change materials (pcms) based cooling. *Solar Energy Materials and Solar Cells*, *241*, 111739. https://www.sciencedirect.com/science/article/pii/S092702482200160X doi: https://doi.org/10.1016/j.solmat.2022.111739

Fudholi, A., and et al. (2014). Performance analysis of photovoltaic thermal (pvt) water collectors. *Energy Conversion and Management*, *78*, 641-651. https://www.sciencedirect.com/science/article/pii/S0196890413007383 doi: https://doi.org/10.1016/j.enconman.2013.11.017

Fujii, T., and Imura, H. (1972). Natural-convection heat transfer from a plate with arbitrary inclination. *Internation Journal of Heat and Mass Transfer*, *15*, 755-764. https://www-sciencedirect-com.tudelft.idm.oclc.org/science/article/pii/0017931072901184?via%3Dihub doi: https://doi.org/10.1016/0017-9310(72)90118-4

Han, X. (2020). Performance improvement of a pv/t system utilizing ag/coso4-propylene glycol nanofluid optical filter. *Energy*, *192*, 116611. https://www.sciencedirect.com/science/article/pii/S0360544219323060 doi: https://doi.org/10.1016/j.energy.2019.116611

Huide, F., and et al. (2017). A comparative study on three types of solar utilization technologies for buildings: Photovoltaic, solar thermal and hybrid photovoltaic/thermal systems. *Energy Conversion and Management*, *140*, 1-13. https://www.sciencedirect.com/science/article/pii/S019689041730170X doi: https://doi.org/10.1016/j.enconman.2017.02.059

Jarimi, H., and et al. (2016). Bi-fluid photovoltaic/thermal (pv/t) solar collector: Experimental validation of a 2-d theoretical model. *Renewable Energy*, *85*, 1052-1067. https://www.sciencedirect.com/science/article/pii/S0960148115301117 doi: https://doi.org/10.1016/j.renene.2015.07.014

Jia, Y., and et al. (2019). Development and applications of photovoltaic–thermal systems: A review. *Renewable and Sustainable Energy Reviews*, *102*, 249-265. https://www.sciencedirect.com/science/article/pii/S1364032118308256 doi: https://doi.org/10.1016/j.rser.2018.12.030

Jin. (2010, Feb). Evaluation of single-pass photovoltaic-thermal air collector with rectangle tunnel absorber. *American Journal of Applied Sciences*, *7*, 277-282. https://thescipub.com/abstract/ajassp.2010.277.282 doi: 10.3844/ajassp.2010.277.282

JinkoSolar. (2017). 72 cheetah hc 72m-v datasheet. https://www.solar4all.eu/wp-content/uploads/2022/12/5d1ad4494a458.pdf

Ju, X. (2020). A fully coupled numerical simulation of a hybrid concentrated photovoltaic/thermal system that employs a therminol vp-1 based nanofluid as a spectral beam filter. *Applied Energy*, *264*, 114701. https://www.sciencedirect.com/science/article/pii/S0306261920302130 doi: https://doi.org/10.1016/j.apenergy.2020.114701

Kalogirou, S. A. (2014). *Solar energy engineering (second edition)* (Second Edition ed.). Boston: Academic Press. https://www.sciencedirect.com/science/article/pii/B9780123972705000066 doi: https://doi.org/10.1016/B978-0-12-397270-5.00006-6

Kazemian, A., and et al. (2020). A year-round study of a photovoltaic thermal system integrated with phase change material in shanghai using transient model. *Energy Conversion and Management*, *210*, 112657. https://www.sciencedirect.com/science/article/pii/S0196890420301953 doi: https://doi.org/10.1016/j.enconman.2020.112657

MathWorks. (2021). *Matlab version: 9.13.0 (r2021a).* Natick, Massachusetts, United States: The MathWorks Inc. https://www.mathworks.com

Or, A. B. (2014). Dependence of multi-junction solar cells parameters on concentration and temperature. *Solar Energy Materials and Solar Cells*, *130*, 234-240. https://www.sciencedirect.com/science/article/pii/S0927024814003717 doi: https://doi.org/10.1016/j.solmat.2014.07.010

Sathe, T. M., and Dhoble, A. (2017). A review on recent advancements in photovoltaic thermal techniques. *Renewable and Sustainable Energy Reviews*, *76*, 645-672. https://www.sciencedirect.com/science/article/pii/S1364032117304136 doi: https://doi.org/10.1016/j.rser.2017.03.075

Shockley, W., and Queisser, H. J. (2004, 06). Detailed Balance Limit of Efficiency of p-n Junction Solar Cells. *Journal of Applied Physics*, *32*(3), 510-519. https://doi.org/10.1063/1.1736034 doi: 10.1063/1.1736034

Singh, P. (2012). Temperature dependence of solar cell performance—an analysis. *Solar Energy Materials and Solar Cells*, *101*, 36-45. https://www.sciencedirect.com/science/article/pii/S0927024812000931 doi: https://doi.org/10.1016/j.solmat.2012.02.019

Smets, A., and et al. (2016). *Solar energy.* UIT Cambridge Ltd.

Solanki, S. (2009). Indoor simulation and testing of photovoltaic thermal (pv/t) air collectors. *Applied Energy*, *86*(11), 2421-2428. https://www.sciencedirect.com/science/article/pii/S0306261909000889 doi: https://doi.org/10.1016/j.apenergy.2009.03.013

SunPower. (2016). 96 x-series residential solar panels datasheet. https://static.trinasolar.com/sites/default/files/PS-M-0473%20C%20Datasheet_Duomax%20M%20Plus_DEG14.XX%28II%29_Sep2017.pdf

Tiwari, G. N. (2002). *Solar energy: fundamentals, design, modelling and applications.* Alpha Science Int'l Ltd.

TrinaSolar. (2017). 72 cell doumax m plus datasheet. https://static.trinasolar.com/sites/default/files/PS-M-0473%20C%20Datasheet_Duomax%20M%20Plus_DEG14.XX%28II%29_Sep2017.pdf

Tyagi, V., and et al. (2012). Advancement in solar photovoltaic/thermal (pv/t) hybrid collector technology. *Renewable and Sustainable Energy Reviews*, *16*(3), 1383-1398. https://www.sciencedirect.com/science/article/pii/S1364032111006058 doi: https://doi.org/10.1016/j.rser.2011.12.013

Vogt, M., Tobon, C. R., Alcañiz, A., Procel, P., Blom, Y., El Din, A. N., ... Isabella, O. (2022). Introducing a comprehensive physics-based modelling framework for tandem and other pv systems. *Solar Energy Materials and Solar Cells*, *247*, 111944. https://www.sciencedirect.com/science/article/pii/S0927024822003622 doi: https://doi.org/10.1016/j.solmat.2022.111944

Wu, S.-Y. (2011). A heat pipe photovoltaic/thermal (pv/t) hybrid system and its performance evaluation. *Energy and Buildings*, *43*(12), 3558-3567. https://www.sciencedirect.com/science/article/pii/S0378778811004051 doi: https://doi.org/10.1016/j.enbuild.2011.09.017

Wu, S.-Y., and et al. (2011). A heat pipe photovoltaic/thermal (pv/t) hybrid system and its performance evaluation. *Energy and Buildings*, *43*(12), 3558-3567. https://www.sciencedirect.com/science/article/pii/S0378778811004051 doi: https://doi.org/10.1016/j.enbuild.2011.09.017

Zhang, X., and et al. (2012). Review of r&d progress and practical application of the solar photovoltaic/thermal (pv/t) technologies. *Renewable and Sustainable Energy Reviews*, *16*(1), 599-617. https://www.sciencedirect.com/science/article/pii/S1364032111004369 doi: https://doi.org/10.1016/j.rser.2011.08.026

Zondag, H. (2002). The thermal and electrical yield of a pv-thermal collector. *Solar Energy*, *72*(2), 113-128. https://www.sciencedirect.com/science/article/pii/S0038092X01000949 doi: https://doi.org/10.1016/S0038-092X(01)00094-9

Zondag, H. (2003). The yield of different combined pv-thermal collector designs. *Solar Energy*, *74*(3), 253-269. https://www.sciencedirect.com/science/article/pii/S0038092X0300121X doi: https://doi.org/10.1016/S0038-092X(03)00121-X

Appendix A

Heat transfer equations

unsteady heat transfer

$$\begin{aligned} T(y,x,z)^{n+1} =& \gamma_{XY}(y,x,z) \cdot T(y,x,z) \\ &+ 2 \cdot Fo_X(y,x,z) \cdot (Bi_X(y,x,z) \cdot T(y,x+1,z) + T(y,x-1,z)) \\ &+ 2 \cdot Fo_Y(y,x,z) \cdot (Bi_Y(y,x,z) \cdot T(y+1,x,z) + T(y-1,x,z)) \\ &+ Fo_Z(y,x,z) \cdot (T(y,x,z+1) + T(y,x,z-1)) \end{aligned} \tag{A.1}$$

$$\begin{aligned} T(y,x,z)^{n+1} =& \gamma_{XYZ}(y,x,z) \cdot T(y,x,z) \\ &+ 2 \cdot Fo_X(y,x,z) \cdot (Bi_X(y,x,z) \cdot T(y,x+1,z) + T(y,x-1,z)) \\ &+ 2 \cdot Fo_Y(y,x,z) \cdot (Bi_Y(y,x,z) \cdot T(y+1,x,z) + T(y-1,x,z)) \\ &+ 2 \cdot Fo_Z(y,x,z) \cdot (Bi_Z(y,x,z) \cdot T(y,x,z+1) + T(y,x,z-1)) \end{aligned} \tag{A.2}$$

$$\beta(y,x,z) = 1 - \left(\frac{\Delta t \cdot k_{material}}{\rho_{material} \cdot Cp_{material}} \right) \cdot \left(\frac{2}{dx^2} + \frac{2}{dy^2} + \frac{2}{dz^2} \right) \tag{A.3}$$

$$Fo_X(y,x,z) = \frac{\Delta t \cdot k_{material}}{\rho_{material} \cdot Cp_{material} \cdot dx^2} \tag{A.4}$$

$$Bi_X(y,x,z) = \frac{h_c \cdot dx^2}{k_{material}} \tag{A.5}$$

$$\begin{aligned} \gamma_X(y,x,z) 1 &- 2 \cdot Fo_X(y,x,z) - 2 \cdot Fo_Y(y,x,z) - 2 \cdot Fo_Z(y,x,z) \\ &- 2 \cdot Fo_X(y,x,z) \cdot Bi_X(y,x,z) \end{aligned} \tag{A.6}$$

$$\begin{aligned} \gamma_{XY}(y,x,z) 1 &- 2 \cdot Fo_X(y,x,z) - 2 \cdot Fo_Y(y,x,z) - 2 \cdot Fo_Z(y,x,z) \\ &- 2 \cdot Fo_X(y,x,z) \cdot Bi_X(y,x,z) \\ &- 2 \cdot Fo_Y(y,x,z) \cdot Bi_Y(y,x,z) \end{aligned} \tag{A.7}$$

$$\begin{aligned}\gamma_{XYZ}(y,x,z) =& 1 - 2 \cdot Fo_X(y,x,z) - 2 \cdot Fo_Y(y,x,z) - 2 \cdot Fo_Z(y,x,z) \\ & - 2 \cdot Fo_X(y,x,z) \cdot Bi_X(y,x,z) \\ & - 2 \cdot Fo_Y(y,x,z) \cdot Bi_Y(y,x,z) \\ & - 2 \cdot Fo_Z(y,x,z) \cdot Bi_Z(y,x,z)\end{aligned} \tag{A.8}$$

steady heat transfer

$$\begin{aligned}T(y,x,z)^{n+1} =& \left(\frac{1}{\frac{3}{dx^2} + \frac{3}{dy^2} + \frac{2}{dz^2}} \right) \cdot \\ & \left(\frac{2 \cdot Tb_X(y,x,z) + T(y,x-1,z)}{dx^2} + \frac{2 \cdot Tb_Y(y,x,z) + T(y-1,x,z)}{dy^2} \right. \\ & \left. + \frac{T(y,x,z+1) + T(y,x,z-1)}{dz^2} \right)\end{aligned} \tag{A.9}$$

$$\begin{aligned}T(y,x,z)^{n+1} =& \left(\frac{1}{\frac{2}{dx^2} + \frac{4}{dy^2} + \frac{2}{dz^2}} \right) \cdot \\ & \left(\frac{T(y,x+1,z) + T(y,x-1,z)}{dx^2} + \frac{2 \cdot Tb_{Yup}(y,x,z) + 2 \cdot Tb_{Ydown}(y,x,z)}{dy^2} \right. \\ & \left. + \frac{T(y,x,z+1) + T(y,x,z-1)}{dz^2} \right)\end{aligned} \tag{A.10}$$

Double border convection

$$\begin{aligned}T(y,x,z)^{n+1} =& k(y,x,z) \cdot \left(\frac{1}{\left(\frac{1}{dx^2} + \frac{1}{dy^2} + \frac{1}{dz^2} \right) \cdot k(y,x,z) + hc \left(\frac{1}{dx} + \frac{1}{dy} \right)} \right) \cdot \\ & \left(hc \cdot \left(\frac{T(y,x+1,z)}{dX} + \frac{T(y+1,x,z)}{dy} \right) + \frac{T(y,x-1,z)}{dx^2} + \right. \\ & \left. \frac{T(y-1,x,z)}{dy^2} + \frac{T(y,x,z+1) + T(y,x,z-1)}{2 \cdot dz^2} \right)\end{aligned} \tag{A.11}$$

Triple border convection

$$\begin{aligned}T(y,x,z)^{n+1} =& k(y,x,z) \cdot \left(\frac{1}{\left(\frac{1}{dx^2} + \frac{1}{dy^2} + \frac{1}{dz^2} \right) \cdot k(y,x,z) + hc \left(\frac{1}{dx} + \frac{1}{dy} + \frac{1}{dz} \right)} \right) \cdot \\ & \left(hc \cdot \left(\frac{T(y,x+1,z)}{dx} + \frac{T(y-1,x,z)}{dy} + \frac{T(y,x,z+1)}{dz} \right) + \right. \\ & \left. \frac{T(y,x-1,z)}{dx^2} + \frac{T(y+1,x,z)}{dy^2} + \frac{T(y,x,z-1)}{dz^2} \right)\end{aligned} \tag{A.12}$$

Collector top loss equations

$$Ra_{air} = \frac{Pr \cdot g \cdot \beta_{air} \cdot (T_{PV} - T_{topglass}) \cdot L_c^3}{\nu_{air}^2} \tag{A.13}$$

$$Ra_{wind} = \frac{Pr \cdot g \cdot \beta_{air} \cdot (T_{topglass} - T_{ambient}) \cdot L_c^3}{\nu_{air}^2} \tag{A.14}$$

$$Ra_{crit} = 10^8 \tag{A.15}$$

Nusselt number for normal convection from PV layer to airgap
Duffie and Beckman (2013)

$$Nu_{air} = 1 + 1.44 \left[1 - \frac{1708 sin(1.8\varphi)^{1.6}}{Ra_{air} \cdot cos(\varphi)}\right] \cdot \left[1 - \frac{1708}{Ra_{air} \cdot cos(\varphi)}\right]^+ + \left[\left(\frac{Ra_{air} \cdot cos(\varphi)}{5830}\right)^{0.333} - 1\right]^+ \tag{A.16}$$

Nusselt number for normal convection from topglass layer to the environment
Fujii and Imura (1972)

$$Nu_{wind} = 0.56(Ra_{crit} cos(\varphi))^{0.25} + 0.13(Ra^{0.333} - Ra_{crit}^{0.333}) \tag{A.17}$$